THE BELL SYSTEM TECHNICAL JOURNAL
Vol. 53, No. 5, May–June 1974
Printed in U.S.A.

Spectra of Digital Phase Modulation by Matrix Methods

By V. K. PRABHU and H. E. ROWE

(Manuscript received October 31, 1973)

We derive the spectral density of a sinusoidal carrier phase modulated by a random baseband pulse train in which the signaling pulse duration is finite and the signaling pulses may have different shapes. The spectral density is expressed as a compact Hermitian form in which the Hermitian matrix is a function of only the symbol probability distribution, and the associated column vector is a function of only the signal pulse shapes. If the baseband pulse duration is longer than one signaling interval, we assume that the symbols transmitted during different time slots are statistically independent. The applicability of the method to compute the spectral density is illustrated by examples for binary, quaternary, octonary, and 16-ary PSK systems with different pulse overlap. Similar methods yield the spectral density of the output of a nonlinear device whose input is a random baseband pulse train with overlapping pulses.

I. INTRODUCTION

In recent years, digital phase-modulation techniques have been playing an increasingly important role in the transmission of information in radio and waveguide systems. Various methods have been developed recently for computing spectra of a sinusoidal carrier phase modulated by a random baseband pulse train.[1–8]

In this paper, we derive the spectral density of a carrier phase modulated by a random baseband pulse stream in which the signaling pulse duration is finite and the signaling pulses may have different shapes. The spectral density is expressed as a compact Hermitian form in which the Hermitian matrix is a function of only the symbol probability distribution and the associated column vector is a function of only the signal pulse shapes. If the baseband pulse duration is longer than one signaling interval and the pulses from different time slots overlap, we assume that the symbols transmitted during different time slots are statistically independent.

The present method also yields the spectral density of the output of a nonlinear device whose input is a similar baseband pulse train.

The work reported here generalizes and simplifies prior results. The form of the present results provides an appropriate division between analysis and machine computation that enhances physical understanding and simplifies numerical computations. We compute the spectra of binary, quaternary, octonary, and 16-ary PSK systems, with overlapping baseband modulation pulses of several shapes.

II. M-ARY PHASE-MODULATED SIGNALS

We seek the spectrum of the digital phase-modulated wave

$$x(t) = \cos[2\pi f_c t + \phi(t)], \quad f_c > 0, \tag{1}$$

where

$$\phi(t) = \sum_{k=-\infty}^{\infty} g_{s_k}(t - kT), \quad s_k = 1, 2, \cdots, M. \tag{2}$$

The discrete random process s_k is assumed strictly stationary; as noted in (2), it takes on only integer values from 1 to M. The carrier frequency is f_c. The signaling alphabet consists of M time functions, $g_1, g_2, \cdots, g_M$, that may have different shapes; one of these is transmitted for each signaling interval T, to generate the digital baseband phase modulation $\phi(t)$. The different signaling waveforms in (2) may overlap, and may be statistically dependent throughout the present section and Appendix A.

For convenience, we define[9]

$$v(t) \equiv e^{j\phi(t)}; \tag{3}$$

then

$$x(t) = \text{Re}\,\{e^{j2\pi f_c t}\, v(t)\}. \tag{4}$$

Appendix A shows that the spectrum of $x(t)$ is

$$\mathbf{P}_x(f) = \tfrac{1}{4}\mathbf{P}_v(f - f_c) + \tfrac{1}{4}\mathbf{P}_v(-f - f_c), \qquad 2f_c \neq \frac{n}{T}, \quad n = 1, 2, 3, \cdots, \tag{5}$$

where[9]

$$\mathbf{P}_v(f) = \int_{-\infty}^{\infty} \Phi_v(\tau) e^{-j2\pi f\tau} d\tau, \tag{6}$$

$$\Phi_v(\tau) = \overline{\Phi_v(t, \tau)} \equiv \lim_{A\to\infty} \frac{1}{2A} \int_{-A}^{A} \Phi_v(t, \tau) dt, \tag{7}^{\dagger}$$

$$\Phi_v(t, \tau) = \langle v(t + \tau) v^*(t) \rangle = \langle e^{j[\phi(t+\tau) - \phi(t)]} \rangle. \tag{8}$$

† The symbol $\overline{}$ denotes average on t throughout.

The first term of (5) is the spectrum of the complex baseband wave $v(t)$ shifted to the carrier frequency $+f_c$; the second term is the spectrum of $v^*(t)$ shifted to $-f_c$. The spectral relationship of (5) is strictly true as long as the condition on f_c is satisfied, whether or not the two spectral terms overlap; that is, this result applies strictly to both narrow-band [$f_c \gg$ bandwidth of $\mathbf{P}_v(f)$] and wideband modulated waves.

The condition of (5) requires that twice the carrier frequency is not an integral multiple of the signaling rate $1/T$. $\mathbf{P}_v(f)$ has in general both continuous and line spectra, the lines occurring at frequencies n/T for integer n. The condition in (5) guarantees that the line components of the two spectral terms never coincide. In the exceptional case, where the two sets of lines do coincide, it is not surprising that it no longer suffices merely to add powers of the two terms, as in (5); however, if f_c is high enough the modulated wave is narrow band, the two spectral terms of (5) do not overlap significantly, and (5) provides a good approximation even if the condition is violated.

Note that we have not found it necessary to randomize the phase of the unmodulated carrier or the position of the time slots of the digital modulation, as is done in various other studies. Thus, rather than (1) we might have considered

$$x(t) = \cos [2\pi f_c t + \phi(t - t_0) + \phi_0], \tag{9}$$

with $\phi(t)$ still given by (2). The spectral relation of (5) will again be strictly true when $2f_cT$ = integer if ϕ_0 and t_0 are independent, and either is uniformly distributed over a suitable interval (Appendix A). However, we retain the original formulation of (1) and (2) throughout —corresponding to $\phi_0 = 0$, $t_0 = 0$ in (9)—to determine the effect of deterministic carrier and modulation phase on the statistics of the modulated wave.

Consequently, we study only $\mathbf{P}_v(f)$ throughout the remainder of this paper. This suffices for all cases except a low carrier frequency f_c that is a precise multiple of half the baud rate $1/2T$; the additional calculations necessary for this exceptional case are suggested in Appendix A, but not carried out in detail.

III. NOTATION AND STATISTICAL MODEL

The introduction of vector-matrix notation greatly simplifies the ensuing analysis.

---

† Either of the two parameters, ϕ_0 or t_0, shifts the relative phase between carrier and modulation; thus, only one of them is really necessary.

First, we rewrite the phase modulation of (2) as

$$\phi(t) = \sum_{k=-\infty}^{\infty} [a_k^{(1)} g_1(t - kT) + a_k^{(2)} g_2(t - kT) + \cdots + a_k^{(M)} g_M(t - kT)]. \quad (10)$$

For a given k (i.e., for a given time slot), one of the a_k's is unity and the rest are zero;

$$\begin{aligned} a_k^{(s_k)} &= 1, \\ a_k^{(i)} &= 0, \quad i \neq s_k, \end{aligned} \quad (11)$$

where s_k is the strictly stationary, discrete random process of (2), taking on the integer values 1, 2, $\cdots$, M.

Now we define for convenience the row vectors

$$\begin{aligned} \underline{\mathbf{a}_k} &\equiv [a_k^{(1)} \; a_k^{(2)} \; \cdots \; a_k^{(M)}], \\ \underline{\mathbf{g}(t)} &\equiv [g_1(t) \; g_2(t) \; \cdots \; g_M(t)], \end{aligned} \quad (12)^{\dagger}$$

whose components are respectively the coefficients and pulse shapes of (10). The transposes[‡] of these row vectors are the column vectors

$$\mathbf{a}_k] = \underline{\mathbf{a}_k}' = \begin{bmatrix} a_k^{(1)} \\ a_k^{(2)} \\ \vdots \\ a_k^{(M)} \end{bmatrix}, \quad \mathbf{g}(t)] = \underline{\mathbf{g}(t)}' = \begin{bmatrix} g_1(t) \\ g_2(t) \\ \vdots \\ g_M(t) \end{bmatrix}. \quad (13)$$

Define the unit basis row vectors

$$\begin{aligned} \underline{\mathbf{e}_1} &\equiv [1 \; 0 \; 0 \; \cdots \; 0], \\ \underline{\mathbf{e}_2} &\equiv [0 \; 1 \; 0 \; \cdots \; 0], \\ &\vdots \\ \underline{\mathbf{e}_M} &\equiv [0 \; 0 \cdots \; 0 \; 1], \end{aligned} \quad (14)$$

with corresponding transpose column vectors $\mathbf{e}_1]$, $\mathbf{e}_2]$, $\cdots$, $\mathbf{e}_M]$. Then $\underline{\mathbf{a}_k}$ takes on only the values $\underline{\mathbf{e}_1}$, $\underline{\mathbf{e}_2}$, $\cdots$, $\underline{\mathbf{e}_M}$ by (11):

$$\underline{\mathbf{a}_k} = \underline{\mathbf{e}_{s_k}}. \quad (15)$$

Now we rewrite (10) in vector notation as

$$\phi(t) = \sum_{k=-\infty}^{\infty} \underline{\mathbf{a}_k} \cdot \mathbf{g}(t - kT)], \quad (16)$$

where $\cdot$ signifies ordinary matrix multiplication throughout. The term

---

† Boldface quantities denote matrices throughout. Row and column vectors are distinguished by the additional notation $\sqcup$ and], respectively.

‡ The transpose of a matrix is indicated by the symbol $'$.

$\underline{\mathbf{a}_k}$ is a vector-valued, discrete† random process, strictly stationary by the assumed strict stationarity of s_k of (2). We define the first- and second-order probabilities of $\underline{\mathbf{a}_k}$ or $\mathbf{a}_k]$ as

$$w_i = \Pr\{\mathbf{a}_k = \mathbf{e}_i\} = \Pr\{s_k = i\} \geqq 0. \tag{17}$$‡

$$W_n(i, j) \equiv \Pr\{\mathbf{a}_k = \mathbf{e}_i, \mathbf{a}_{k+n} = \mathbf{e}_j\} = \Pr\{s_k = i, s_{k+n} = j\} \geqq 0. \tag{18}$$‡

w_i is the probability that the ith signaling waveform g_i is transmitted in any time slot, $W_n(i, j)$ the joint probability that the signaling waveforms g_i and g_j are transmitted in two time slots separated by n signaling intervals. w_i and $W_n(i, j)$ are independent of k by the assumption of stationarity. Then since the marginal probabilities are obtained by summing over the joint probability function,

$$\sum_{i=1}^{M} W_n(i, j) = w_j, \quad \sum_{j=1}^{M} W_n(i, j) = w_i. \tag{19}$$

Normalization of the total probability to 1 requires

$$\sum_{i=1}^{M} w_i = 1, \quad \sum_{i=1}^{M} \sum_{j=1}^{M} W_n(i, j) = 1. \tag{20}$$

Now we introduce vector-matrix notation for the probabilities. Let

$$\underline{\mathbf{w}} \equiv [w_1 \; w_2 \cdots w_M] \tag{21}$$

be the probability row vector whose elements give the probabilities of the different signaling waveforms, with transpose column vector

$$\mathbf{w}] = \underline{\mathbf{w}}'. \tag{22}$$

Let

$$\mathbf{W}_n \equiv \begin{bmatrix} W_n(1, 1) & W_n(1, 2) & \cdots & W_n(1, M) \\ W_n(2, 1) & W_n(2, 2) & \cdots & W_n(2, M) \\ \vdots & \vdots & \cdots & \vdots \\ W_n(M, 1) & W_n(M, 2) & \cdots & W_n(M, M) \end{bmatrix} \tag{23}$$

be the matrix whose elements specify the joint probabilities of all pairs of signaling waveforms separated by n time slots. Further, define

$$\underline{\mathbf{1}} = \mathbf{1}]' \equiv [1 \; 1 \cdots 1] \tag{24}$$

as a vector with all M elements unity. Then (19) and (20) may be written as

$$\underline{\mathbf{1}} \cdot \mathbf{W}_n = \underline{\mathbf{w}}, \qquad \mathbf{W}_n \cdot \mathbf{1}] = \mathbf{w}] \tag{25}$$

---

† $\underline{\mathbf{a}_k}$ is defined only for integer values of its independent variable k.

‡ It is understood that $\mathbf{a}$, $\mathbf{e}$ are either row or column vectors throughout (17) and (18), and in succeeding equations.

and

$$\underline{1}\cdot\mathbf{w}\rceil = \underline{\mathbf{w}}\cdot\mathbf{1}\rceil = 1, \qquad \underline{1}\cdot\mathbf{W}_n\cdot\mathbf{1}\rceil = 1. \tag{26}$$

The probability matrices have the following useful properties. For $n = 0$, the joint probability matrix of (23) and (18) is diagonal, with diagonal elements the first-order symbol probabilities;

$$\mathbf{W}_0 = \begin{bmatrix} w_1 & & & 0 \\ & w_2 & & \\ & & \ddots & \\ 0 & & & w_M \end{bmatrix} \equiv \mathbf{w}_d, \tag{27}$$

where we define the diagonal matrix $\mathbf{w}_d$ for later convenience. Then

$$\mathbf{w}_d\cdot\mathbf{1}\rceil = \mathbf{w}\rceil, \quad \underline{1}\cdot\mathbf{w}_d = \underline{\mathbf{w}}. \tag{28}$$

By symmetry,

$$W_n(i, j) = W_{-n}(j, i), \tag{29}$$

or in matrix notation

$$\mathbf{W}_n = \mathbf{W}_{-n}{}'. \tag{30}$$

We assume that signaling waveforms in widely separated time slots are statistically independent:

$$\lim_{n\to\infty} W_n(i, j) = w_i w_j, \tag{31}$$

or in matrix form

$$\lim_{n\to\infty} \mathbf{W}_n = \mathbf{w}\rceil\cdot\underline{\mathbf{w}}. \tag{32}$$

Since

$$(\mathbf{w}\rceil\cdot\underline{\mathbf{w}})' = \mathbf{w}\rceil\cdot\underline{\mathbf{w}}, \tag{33}$$

(30) and (32) yield

$$\mathbf{W}_\infty = \mathbf{W}_\infty{}' = \mathbf{W}_{-\infty}. \tag{34}$$

Using the above, the mean and covariance of the strictly stationary, vector-valued, discrete random process $\mathbf{a}_k$ are

$$\langle\mathbf{a}_k\rceil = \mathbf{w}\rceil, \quad \langle\underline{\mathbf{a}_k}\rangle = \underline{\mathbf{w}}, \tag{35}$$

$$\tilde{\mathbf{\Phi}}_{\mathbf{a}}(n) \equiv \langle\mathbf{a}_{k+n}\rceil\cdot\underline{\mathbf{a}_k}\rangle = \mathbf{W}_n. \tag{36}$$

The assumption of independence in (31) and (32) implies uncorrelation in (36) as $n \to \infty$. Conversely, uncorrelation implies independence, because the random vectors $\mathbf{a}_k$ are unit basis vectors (15),[10] rendering the covariance and probability matrices identical. Thus, rather than assuming independence in (31) and (32), we might equally well assume that the modulation vectors $\mathbf{a}_k$ become uncorrelated for widely separated time slots.

The spectral density of $\mathbf{a}_k$ is the discrete transform of (36);

$$\tilde{\mathbf{P}}_{\mathbf{a}}(f) = \sum_{n=-\infty}^{\infty} e^{-j2\pi fn}\mathbf{W}_n. \tag{37}^{\dagger}$$

Equations (36) and (37) are the matrix extensions for discrete vector random processes of similar scalar relations for discrete scalar random processes;[11] the symbol ~ indicates that a discrete random process is under consideration. We separate (37) into line and continuous spectral components:

$$\tilde{\mathbf{P}}_{\mathbf{a}}(f) = \tilde{\mathbf{P}}_{\mathbf{a}_l}(f) + \tilde{\mathbf{P}}_{\mathbf{a}_c}(f). \tag{38}$$

Then from (32) and (37):

$$\tilde{\mathbf{P}}_{\mathbf{a}_l}(f) = \mathbf{w}]\cdot\underline{\mathbf{w}}\sum_{n=-\infty}^{\infty} \delta(f-n), \tag{39}$$

$$\tilde{\mathbf{P}}_{\mathbf{a}_c}(f) = \sum_{n=-\infty}^{\infty} e^{-j2\pi fn}\{\mathbf{W}_n - \mathbf{w}]\cdot\underline{\mathbf{w}}\}. \tag{40}$$

The assumption of (31) and (32) that signaling waveforms in widely separated time slots are independent, or the equivalent assumption that $\mathbf{a}_{k+n}$ and $\mathbf{a}_k$ become uncorrelated for large n, eliminates line components except dc if we confine our attention to the fundamental frequency interval $|f| < \frac{1}{2}$, and so retain only the $n = 0$ term in (39).[‡] Consequently, the modulation has no periodic patterns.

IV. PSK AS A BASEBAND PULSE TRAIN

Our problem has been reduced to determining the spectral density of the complex wave $v(t)$:

$$v(t) \equiv e^{j\phi(t)}, \tag{41}$$

$$\phi(t) = \sum_{k=-\infty}^{\infty} \underline{\mathbf{a}_k}\cdot\mathbf{g}(t-kT)], \tag{42}$$

where $\mathbf{a}$ and $\mathbf{g}$ are M-dimensional vectors. We show that if the signaling pulses are strictly time-limited to an interval KT, $v(t)$ may be written

$$v(t) = \sum_{k=-\infty}^{\infty} \underline{\mathbf{b}_k}\cdot\mathbf{r}(t-kT)]. \tag{43}$$

---

† While this relation is defined for the entire range $-\infty < f < \infty$, $\tilde{\mathbf{P}}_{\mathbf{a}}(f)$ is periodic in f with unit period, and only the fundamental period $|f| < \frac{1}{2}$ is normally of interest. Thus, the inverse transform is

$$\tilde{\mathbf{\Phi}}_{\mathbf{a}}(n) = \mathbf{W}_n = \int_{-\frac{1}{2}}^{\frac{1}{2}} \tilde{\mathbf{P}}_{\mathbf{a}}(f)e^{+j2\pi fn}df.$$

‡ We may thus write $\mathbf{a}_k = \mathbf{w} + \mathbf{a}_{ck}$ with (40) giving the spectral density of $\mathbf{a}_c$ and (39) the spectral density of $\mathbf{w}$.

Vectors $\mathbf{b}$ and $\mathbf{r}$ are M^K-dimensional vectors expressed in terms of $\mathbf{a}$ and $\mathbf{g}$, respectively. The different terms in (43) are strictly nonoverlapping:

$$\mathbf{r}(t)] = \mathbf{0}], \quad t \leqq 0, \quad t > T. \tag{44}$$†

Each $\mathbf{b}_k$ is a unit basis vector, i.e., only one of its M^K components is unity, all others being zero. The spectral density of (43) is determined in Appendix B.

Figure 1 shows portions of $\phi(t)$ of (42) for four different maximum signal pulse durations; the terms $k = -1, 0, 1, 2$ of (42) are shown, and for convenience $\mathbf{a}_k$ has been taken the same for each of these time slots. The pulses are positioned along the time slots such that the limits of each signal pulse lie on the boundary between adjacent time slots (i.e., $t = \text{integer} \cdot T$); since symmetric pulses have been chosen for illustration in Fig. 1, their maxima are centered in the time slots for K odd, and lie on the time-slot boundaries for K even. Examine the $(0, T]$ time slot in Fig. 1 as typical; then with the above choice of pulse positions, the number of pulses contributing to $\phi(t)$ in each time slot equals K. Since each pulse can take on M different shapes, $\phi(t)$ can take on M^K different shapes in each time slot; the same is true for $v(t)$ of (41), thus demonstrating the representation of (43).

It remains for us to express the pulse shapes $\mathbf{r}(t)$ and coefficients $\mathbf{b}_k$ of (43) in terms of the signal pulses $\mathbf{g}(t)$ and coefficients $\mathbf{a}_k$ of (42). We give separate treatments for the cases $K = 1$ and $K = 2$, and extend these results to general K.

4.1 Nonoverlapping pulses: $K = 1$

The top portion of Fig. 1 shows digital phase modulation for which the signal pulses in different time slots never overlap; in this case,

$$\mathbf{g}(t)] = \mathbf{0}], \qquad t \leqq 0, \quad t > T, \tag{45}$$

where $\mathbf{0}]$ represents the M-dimensional zero vector. Define

$$\underline{\mathbf{q}(t)} \equiv \begin{cases} [e^{j\theta_1(t)}\ e^{j\theta_2(t)} \cdots e^{j\theta_M(t)}], & 0 < t \leqq T. \\ \underline{0}, & t \leqq 0, \quad t > T. \end{cases} \tag{46}$$

Then (41) and (42) may be written

$$v(t) = \sum_{k=-\infty}^{\infty} \underline{\mathbf{a}_k} \cdot \mathbf{q}(t - kT)]. \tag{47}$$

† $\mathbf{0}] = \underline{0}'$ is a vector of appropriate dimension (here M^K) with all elements zero.

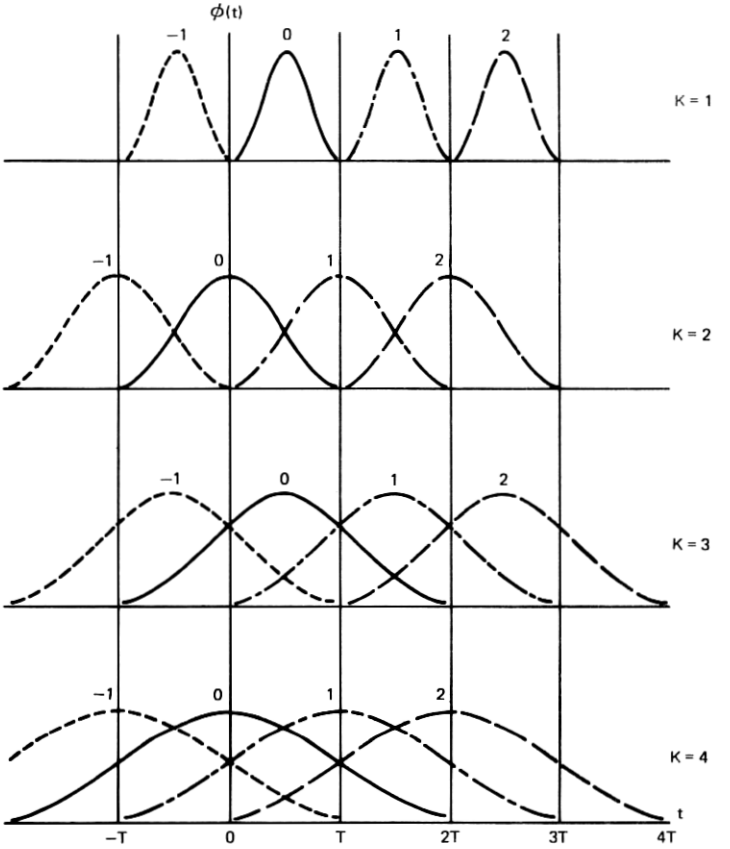

Fig. 1—Phase modulation for different signal pulse durations. Index k [eq. (42)] is shown near peak of each pulse. Also, for simplicity, same signal pulse is shown for each k. T = time slot duration or signaling period. KT = maximum signal pulse duration. Note different pulse center location for odd and even K.

Comparing (47) and (43), the parameters of the latter are given as follows for nonoverlapping signal pulses:

$$\underline{\mathbf{b}}_k = \underline{\mathbf{a}}_k, \quad \mathbf{r}(t)] = \mathbf{q}(t)]; \quad K = 1. \tag{48}$$

4.2 Overlapping pulses: $K = 2$

This case is illustrated in the second portion of Fig. 1. In the $(0, T]$ time slot, the $k = 0, 1$ pulses contribute. We have

$$\mathbf{g}(t)] = 0], \qquad t \leqq -T, \quad t > T. \tag{49}$$

Define

$$\underline{\mathbf{q}(t)} \equiv \begin{cases} [e^{j\vartheta_1(t)}\ e^{j\vartheta_2(t)}\ \cdots\ e^{j\vartheta_M(t)}], & -T < t \leqq T. \\ \underline{0}, & t \leqq -T,\quad t > T. \end{cases} \tag{50}^{\dagger}$$

Then

$$\begin{aligned} v(t) &= \sum_{k=-\infty}^{\infty} \{\underline{\mathbf{a}_k}\cdot\mathbf{q}(t-kT)]\}\{\underline{\mathbf{a}_{k+1}}\cdot\mathbf{q}(t-(k+1)T)]\} \\ &= \sum_{k=-\infty}^{\infty} \{\underline{\mathbf{a}_k}\cdot\mathbf{q}(t-kT)\ ]\} \times \{\underline{\mathbf{a}_{k+1}}\cdot\mathbf{q}(t-(k+1)T]\} \\ &= \sum_{k=-\infty}^{\infty} \{\underline{\mathbf{a}_k} \times \underline{\mathbf{a}_{k+1}}\}\cdot\{\mathbf{q}(t-kT)] \times \mathbf{q}(t-(k+1)T)]\}, \end{aligned} \tag{51}$$

where $\times$ denotes the (right) Kronecker product[12,13] throughout.[‡] Comparing the last line of (51) with (43), the parameters of the latter are given as follows when no more than two signal pulses overlap:

$$\underline{\mathbf{b}_k} = \underline{\mathbf{a}_k} \times \underline{\mathbf{a}_{k+1}},\quad \mathbf{r}(t)] = \mathbf{q}(t)] \times \mathbf{q}(t-T)];\quad K = 2. \tag{52}$$

Since the elements of $\mathbf{b}_k$ consist of all pairs of products of the elements of $\mathbf{a}_k$ and $\mathbf{a}_{k+1}$, and since the $\mathbf{a}_k$ are M-dimensional unit-basis vectors

---

† Comparing (50) with (46), note that the definition of $\mathbf{q}(t)$ is different for different K; $\mathbf{q}(t) \not\equiv 0$ over the same interval in which $\mathbf{g}(t)$ may be nonzero.

‡ The second line of (51) follows from the first by the observation that the two scalars may be regarded as 1-by-1 matrices; consequently, their scalar product and their Kronecker product are identical. The third line follows from the second by the well-known result connecting ordinary matrix and Kronecker products as follows: Consider two arbitrary matrices $\mathbf{A}$ and $\mathbf{B}$ with elements a_{ij}, b_{ij}. Define the (right) Kronecker product by (Refs. 12 and 13):

$$\mathbf{A} \times \mathbf{B} \equiv \begin{bmatrix} a_{11}\mathbf{B} & a_{12}\mathbf{B} & \cdots \\ a_{21}\mathbf{B} & a_{22}\mathbf{B} & \cdots \\ \cdots & \cdots & \cdots \end{bmatrix}$$

The following results may be found in Refs. 12 or 13.

For any matrices $\mathbf{A}$, $\mathbf{B}$, $\mathbf{C}$, and $\mathbf{D}$:

$$\mathbf{A} \times \mathbf{B} \times \mathbf{C} = (\mathbf{A} \times \mathbf{B}) \times \mathbf{C} = \mathbf{A} \times (\mathbf{B} \times \mathbf{C}), \qquad (\mathbf{A} \times \mathbf{B})' = \mathbf{A}' \times \mathbf{B}'.$$

For $\mathbf{A}$ and $\mathbf{B}$ the same size, and $\mathbf{C}$ and $\mathbf{D}$ the same size (possibly different from the size of $\mathbf{A}$ and $\mathbf{B}$):

$$(\mathbf{A} + \mathbf{B}) \times (\mathbf{C} + \mathbf{D}) = \mathbf{A} \times \mathbf{C} + \mathbf{A} \times \mathbf{D} + \mathbf{B} \times \mathbf{C} + \mathbf{B} \times \mathbf{D}.$$

Assume the matrices $\mathbf{A}_1$, $\mathbf{B}_1$ and $\mathbf{A}_2$, $\mathbf{B}_2$ are dimensioned so that the ordinary matrix products $\mathbf{A}_1\cdot\mathbf{B}_1$ and $\mathbf{A}_2\cdot\mathbf{B}_2$ exist (i.e., there are λ columns of $\mathbf{A}_1$ and rows of $\mathbf{B}_1$, and μ columns of $\mathbf{A}_2$ and rows of $\mathbf{B}_2$). Then

$$(\mathbf{A}_1\cdot\mathbf{B}_1) \times (\mathbf{A}_2\cdot\mathbf{B}_2) = (\mathbf{A}_1 \times \mathbf{A}_2)\cdot(\mathbf{B}_1 \times \mathbf{B}_2);$$

this result generalizes to

$$(\mathbf{A}_1\cdot\mathbf{B}_1\cdot\mathbf{C}_1) \times (\mathbf{A}_2\cdot\mathbf{B}_2\cdot\mathbf{C}_2) \times (\mathbf{A}_3\cdot\mathbf{B}_3\cdot\mathbf{C}_3) = (\mathbf{A}_1 \times \mathbf{A}_2 \times \mathbf{A}_3)\cdot(\mathbf{B}_1 \times \mathbf{B}_2 \times \mathbf{B}_3)\cdot(\mathbf{C}_1 \times \mathbf{C}_2 \times \mathbf{C}_3)$$

etc.

by (14) and (15), the $\mathbf{b}_k$ are M^2-dimensional unit-basis vectors: that is, $\mathbf{b}_k$ has one element unity and the remainder $M^2 - 1$ elements zero. Note from (52) and (50) that

$$\mathbf{r}(t)] = \mathbf{0}], \quad t \leqq 0, \quad t > T. \tag{53}$$

We illustrate these relations for the binary case,[14] in which only two signal waveforms $g_1(t)$ and $g_2(t)$ are transmitted. Then

$$\mathbf{g}(t)] \equiv \begin{bmatrix} g_1(t) \\ g_2(t) \end{bmatrix} = \begin{bmatrix} 0 \\ 0 \end{bmatrix}, \qquad t \leqq -T, \quad t > T. \tag{54}$$

$$\mathbf{q}(t)] = \begin{cases} \begin{bmatrix} e^{j\theta_1(t)} \\ e^{j\theta_2(t)} \end{bmatrix}, & -T < t \leqq T. \\ \begin{bmatrix} 0 \\ 0 \end{bmatrix} & t \leqq -T, \quad t > T. \end{cases} \tag{55}$$

$$\mathbf{r}(t)] = \begin{cases} \begin{bmatrix} e^{j[\theta_1(t)+\theta_1(t-T)]} \\ e^{j[\theta_1(t)+\theta_2(t-T)]} \\ e^{j[\theta_2(t)+\theta_1(t-T)]} \\ e^{j[\theta_2(t)+\theta_2(t-T)]} \end{bmatrix}, & 0 < t \leqq T. \\ \begin{bmatrix} 0 \\ 0 \\ 0 \\ 0 \end{bmatrix}, & t \leqq 0, \quad t > T. \end{cases} \tag{56}$$

$$\begin{aligned} \underline{\mathbf{b}}_k &= [a_k^{(1)} \; a_k^{(2)}] \times [a_{k+1}^{(1)} \; a_{k+1}^{(2)}] \\ &= [a_k^{(1)} \; a_{k+1}^{(1)} \;\; a_k^{(1)} \; a_{k+1}^{(2)} \;\; a_k^{(2)} \; a_{k+1}^{(1)} \;\; a_k^{(2)} \; a_{k+1}^{(2)}]. \end{aligned} \tag{57a}$$

$\underline{\mathbf{b}}_k$:

$\underline{\mathbf{a}}_k$ \ $\underline{\mathbf{a}}_{k+1}$	$[1\ 0]$	$[0\ 1]$
$[1\ 0]$	$[1\ 0\ 0\ 0]$	$[0\ 1\ 0\ 0]$
$[0\ 1]$	$[0\ 0\ 1\ 0]$	$[0\ 0\ 0\ 1]$

(57b)

The four possible waveshapes for $\phi(t)$ in the $(0, T]$ time slot are shown in Fig. 2.

4.3 Overlapping pulses: General K

The general case is treated by straightforward extension of the above method; Fig. 1 illustrates the phase modulation for $K = 3, 4$. The following expressions differ slightly for the even and odd cases; they

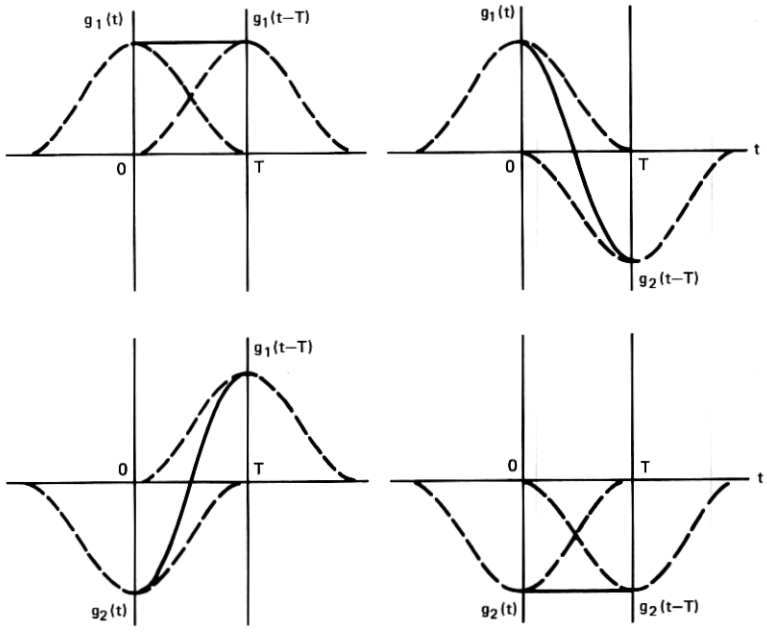

Fig. 2—$\phi(t)$ for $0 < t \leqq T$, binary signaling, and $K = 2$.

correctly reduce to the above results for $K = 1, 2$.

$$\mathbf{g}(t)] = \mathbf{0}], \quad \begin{cases} t \leqq -\dfrac{K-1}{2}T, \quad t > \dfrac{K+1}{2}T; & K \text{ odd.} \\ t \leqq -\dfrac{K}{2}T, \qquad t > \dfrac{K}{2}T; & K \text{ even.} \end{cases} \tag{58}$$

$$\underline{\mathbf{q}(t)} \equiv \begin{cases} [e^{j\underline{g}_1(t)}\, e^{j\underline{g}_2(t)} \cdots e^{j\underline{g}_M(t)}], \\ \quad -\dfrac{K-1}{2}T < t \leqq \dfrac{K+1}{2}T; & K \text{ odd.} \\ \quad -\dfrac{K}{2}T < t \leqq \dfrac{K}{2}T; & K \text{ even.} \\ \underline{\mathbf{0}}, \\ \quad t \leqq -\dfrac{K-1}{2}T, \quad t > \dfrac{K+1}{2}T; & K \text{ odd.} \\ \quad t \leqq -\dfrac{K}{2}T, \quad t > \dfrac{K}{2}T; & K \text{ even.} \end{cases} \tag{59}$$

The parameters of (43) are:

$$\underline{\mathbf{b}}_k = \prod_{i=-(K-1)/2}^{(K-1)/2 \times} \underline{\mathbf{a}}_{k+i}, \quad \mathbf{r}(t)] = \prod_{i=-(K-1)/2}^{(K-1)/2 \times} \mathbf{q}(t - iT)]; \quad K \text{ odd.} \tag{60}^{\dagger}$$

$$\underline{\mathbf{b}}_k = \prod_{i=-(K/2)+1}^{K/2 \times} \underline{\mathbf{a}}_{k+i}, \quad \mathbf{r}(t)] = \prod_{i=-(K/2)+1}^{K/2 \times} \mathbf{q}(t - iT)]; \quad K \text{ even.} \tag{61}^{\dagger}$$

Note that

$$\mathbf{r}(t)] = \mathbf{0}], \qquad t \leqq 0, \quad t > T. \tag{62}$$

V. PSK WITH NONOVERLAPPING, CORRELATED SIGNAL PULSES: $K = 1$

Assume the signal pulses are confined to one time slot, as in (45):

$$\mathbf{g}(t)] = \mathbf{0}], \quad t \leqq 0, \quad t > T. \tag{63}$$

From (46) to (48) and (160) to (161),

$$\mathbf{R}(f)] = \int_0^T e^{-j2\pi ft} \begin{bmatrix} e^{jg_1(t)} \\ e^{jg_2(t)} \\ \vdots \\ e^{jg_M(t)} \end{bmatrix} dt. \tag{64}$$

We separate $v(t)$ of (2) and (3) or (41) and (42) into line and continuous components:

$$v(t) \equiv e^{j\phi(t)} = v_l(t) + v_c(t). \tag{65}$$

Using (48) and comparing (32) to (37) with (149) to (153), we have from (171)

$$v_l(t) = \frac{1}{T} \underline{\mathbf{w}}_{\cdot} \sum_{n=-\infty}^{\infty} \mathbf{R}\left(\frac{n}{T}\right)] e^{jn2\pi t/T}. \tag{66}$$

From (165),

$$\mathbf{P}_{v_l}(f) = \frac{1}{T^2} |\underline{\mathbf{w}}_{\cdot} \mathbf{R}(f)]|^2 \sum_{n=-\infty}^{\infty} \delta\left(f - \frac{n}{T}\right), \tag{67}$$

---

† The symbol $\prod_{\times}$ used here and subsequently indicates a multiple Kronecker product:

$$\prod_{i=L}^{N \times} \mathbf{A}_i \equiv \mathbf{A}_L \times \mathbf{A}_{L+1} \times \cdots \times \mathbf{A}_{N-1} \times \mathbf{A}_N.$$

The products in (60) and (61) contain K factors.

which may be written

$$\mathbf{P}_{v_l}(f) = \frac{1}{T^2}\,|w_1R_1(f) + w_2R_2(f) + \cdots + w_MR_M(f)\,|^2 \cdot \sum_{n=-\infty}^{\infty} \delta\left(f - \frac{n}{T}\right). \quad (68)$$

From (162) and (164)

$$\mathbf{P}_{v_c}(f) = \frac{1}{T}\underline{\mathbf{R}(f)}\cdot \sum_{n=-\infty}^{\infty} e^{-j2\pi fTn}\,\{\mathbf{W}_n - \mathbf{w}]\cdot\underline{\mathbf{w}}\}\cdot\mathbf{R}^*(f)]. \quad (69)$$

We illustrate these general results with two examples.

5.1 Independent, M-ary signal pulses

Equation (32) now holds for all $n \neq 0$; using (21),

$$\mathbf{W}_n = \mathbf{w}]\cdot\underline{\mathbf{w}} \equiv \begin{bmatrix} w_1 \\ w_2 \\ \vdots \\ w_M \end{bmatrix}\cdot[w_1\, w_2 \cdots w_M], \quad n \neq 0. \quad (70)$$

From (27),

$$\mathbf{W}_0 = \mathbf{w}_d \equiv \begin{bmatrix} w_1 & & & 0 \\ & w_2 & & \\ & & \ddots & \\ 0 & & & w_M \end{bmatrix}. \quad (71)$$

Then only the $n = 0$ term remains in (69);

$$\mathbf{P}_{v_c}(f) = \frac{1}{T}\underline{\mathbf{R}(f)}\cdot\mathbf{w}_d\cdot\mathbf{R}^*(f)] - \frac{1}{T}\,|\underline{\mathbf{w}}\cdot\mathbf{R}(f)]\,|^2. \quad (72)$$

Writing out the matrix operations, (72) yields

$$\begin{aligned}\mathbf{P}_{v_c}(f) &= \frac{1}{T}\,[w_1|R_1(f)\,|^2 + w_2|R_2(f)\,|^2 + \cdots + w_M|R_M(f)\,|^2] \\ &\quad - \frac{1}{T}\,|w_1R_1(f) + w_2R_2(f) + \cdots + w_MR_M(f)\,|^2 \\ &= \frac{1}{2T}\sum_{i=1}^{M}\sum_{j=1}^{M} w_i\,w_j|R_i(f) - R_j(f)\,|^2. \end{aligned} \quad (73)$$

This result has been given in Ref. 6. The line component is given by (66), its spectrum by (67) and (68).

5.2 Correlated, binary signal pulses: $M = 2$

The matrix $\mathbf{W}_n$ consists of the four upper left-hand elements of (23). The constraints of (19) and (20) or (25) and (26) render three of these functions dependent on the fourth.

$$W_n = [W_n(1, 1) - w_1^2]\begin{bmatrix} 1 & -1 \\ -1 & 1 \end{bmatrix} + \mathbf{w}]\cdot\underline{\mathbf{w}}. \tag{74}$$

From (27)

$$W_0(1, 1) = w_1, \tag{75}$$

from (30)

$$W_n(1, 1) = W_{-n}(1, 1), \tag{76}$$

and from (31)

$$\lim_{n\to\infty} W_n(1, 1) = w_1^2. \tag{77}$$

Equation (69) becomes

$$\mathbf{P}_{v_c}(f) = \frac{1}{T}\,|R_1(f) - R_2(f)|^2 \sum_{n=-\infty}^{\infty} e^{-j2\pi fTn}[W_n(1, 1) - w_1^2]. \tag{78}$$

$W_n(1, 1)$ may be any discrete covariance function satisfying the constraints of (75) to (77). The line component and its spectrum are again given by (66), (67), and (68) with two-component vectors, e.g.,

$$\mathbf{P}_{v_l}(f) = \frac{1}{T^2}\,|w_1R_1(f) + w_2R_2(f)|^2 \sum_{n=-\infty}^{\infty} \delta\left(f - \frac{n}{T}\right). \tag{79}$$

The binary independent case is obtained by setting

$$W_n(1, 1) = w_1^2, \quad n \neq 0. \tag{80}$$

Then (78) becomes

$$\mathbf{P}_{v_c}(f) = \frac{w_1w_2}{T}\,|R_1(f) - R_2(f)|^2. \tag{81}$$

This agrees with (73) for the binary case.

VI. PSK WITH INDEPENDENT, OVERLAPPING SIGNAL PULSES: $K = 2$

Assume that no more than two signal pulses overlap, as in (49):

$$\mathbf{g}(t)] = 0], \quad t \leqq -T, \quad t > T. \tag{82}$$

$\mathbf{R}(f)$ is determined from (50) to (53) and (160) to (161):

$$\mathbf{R}(f)\rceil = \int_0^T e^{-j2\pi ft} \begin{bmatrix} e^{j[g_1(t)+g_1(t-T)]} \\ \vdots \\ e^{j[g_1(t)+g_M(t-T)]} \\ e^{j[g_2(t)+g_1(t-T)]} \\ \vdots \\ e^{j[g_2(t)+g_M(t-T)]} \\ e^{j[g_3(t)+g_1(t-T)]} \\ \vdots \\ e^{j[g_{M-1}(t)+g_M(t-T)]} \\ e^{j[g_M(t)+g_1(t-T)]} \\ \vdots \\ e^{j[g_M(t)+g_M(t-T)]} \end{bmatrix} dt. \tag{83}$$

From (52),

$$\underline{\mathbf{b}_k} = \underline{\mathbf{a}_k} \times \underline{\mathbf{a}_{k+1}}. \tag{84}$$

We determine the mean and covariance of $\mathbf{b}_k$ from (32) to (37) and (149) to (153). We assume throughout this section that signal pulses in different time slots are independent, as in (70) and (71):

$$\mathbf{W}_0 = \mathbf{w}_d; \quad \mathbf{W}_n = \mathbf{w}\rceil \cdot \underline{\mathbf{w}}, \quad |n| \neq 0. \tag{85}$$

For the mean, since $\mathbf{a}_k$ and $\mathbf{a}_{k+1}$ are independent,

$$\begin{aligned} \underline{\beta} \equiv \langle \underline{\mathbf{b}_k} \rangle &= \underline{\mathbf{w}} \times \underline{\mathbf{w}} \\ &\equiv \underline{\mathbf{w}}^{[2]}. \end{aligned} \tag{86}$$

We introduce the notation that an integer exponent enclosed in square brackets denotes the Kronecker power,[12] i.e., the Kronecker product of the matrix (or vector) with itself the indicated number of times.

For the covariance (see footnote, p. 908):

$$\begin{aligned} \tilde{\mathbf{\Phi}}_{\mathbf{b}}(n) &\equiv \langle \mathbf{b}_{k+n}\rceil \cdot \underline{\mathbf{b}_k} \rangle \\ &= \langle (\mathbf{a}_{k+n}\rceil \times \mathbf{a}_{k+n+1}\rceil) \cdot (\underline{\mathbf{a}_k} \times \underline{\mathbf{a}_{k+1}}) \rangle \\ &= \langle (\mathbf{a}_{k+n}\rceil \cdot \underline{\mathbf{a}_k}) \times (\mathbf{a}_{k+n+1}\rceil \cdot \underline{\mathbf{a}_{k+1}}) \rangle. \end{aligned} \tag{87}$$

Since

$$\tilde{\mathbf{\Phi}}_{\mathbf{b}}(n) = \tilde{\mathbf{\Phi}}'_{\mathbf{b}}(-n), \tag{88}$$

we study only $n \geqq 0$. We treat three cases.

First assume $|n| \geqq 2$. All the $\mathbf{a}$'s in (87) are independent; from the second line,

$$\begin{aligned} \tilde{\mathbf{\Phi}}_{\mathbf{b}}(n) &= (\mathbf{w}\rceil \times \mathbf{w}\rceil) \cdot (\underline{\mathbf{w}} \times \underline{\mathbf{w}}) \\ &= \mathbf{w}\rceil^{[2]} \cdot \underline{\mathbf{w}}^{[2]}, \quad |n| \geqq 2. \end{aligned} \tag{89}$$

Next consider $n = 0$. From the third line of (87) and the fact that $\mathbf{a}_k$ and $\mathbf{a}_{k+1}$ are independent,

$$\tilde{\mathbf{\Phi}}_b(0) = \mathbf{w}_d^{[2]}. \tag{90}$$

Finally, for $|n| = 1$, from the third line of (87) we have† (see footnote, p. 908):

$$\begin{aligned}\tilde{\mathbf{\Phi}}_b(1) &= \langle(\mathbf{a}_{k+1}] \times \underline{\mathbf{a}_k}) \times (\mathbf{a}_{k+2}] \times \underline{\mathbf{a}_{k+1}})\rangle \\ &= \langle\underline{\mathbf{a}_k} \times (\mathbf{a}_{k+1}] \times \underline{\mathbf{a}_{k+1}}) \times \mathbf{a}_{k+2}]\rangle.\end{aligned} \tag{91}$$

Since $\mathbf{a}_k$, $\mathbf{a}_{k+1}$, $\mathbf{a}_{k+2}$ are independent,

$$\tilde{\mathbf{\Phi}}_b(1) = \underline{\mathbf{w}} \times \mathbf{w}_d \times \mathbf{w}]. \tag{92}$$

From (88),

$$\tilde{\mathbf{\Phi}}_b(-1) = \mathbf{w}] \times \mathbf{w}_d \times \underline{\mathbf{w}}. \tag{93}$$

From (86) to (89), (153) is satisfied, i.e., $\mathbf{b}_k$ for widely separated time slots are uncorrelated.‡ Therefore, from (86), (165), and (171):

$$v_l(t) = \frac{1}{T}\underline{\mathbf{w}}^{[2]} \cdot \sum_{n=-\infty}^{\infty} \mathbf{R}\left(\frac{n}{T}\right) e^{jn2\pi t/T}; \tag{94}$$

$$\mathbf{P}_{v_l}(f) = \frac{1}{T^2}\,|\underline{\mathbf{w}}^{[2]} \cdot \mathbf{R}(f)]|^2 \sum_{n=-\infty}^{\infty} \delta(f - nT). \tag{95}$$

In comparing these results with (66) and (67), note that $\mathbf{R}(f)$ of (83) differs from $\mathbf{R}(f)$ of (64).

Substituting (86), (89), (90), (92), and (93) into (162) and (164), the continuous spectrum is

$$\begin{aligned}\mathbf{P}_{v_c}(f) = \frac{1}{T}\underline{\mathbf{R}(f)} \cdot \{&(\mathbf{w}_d^{[2]} - \mathbf{w}]^{[2]} \cdot \underline{\mathbf{w}}^{[2]}) \\ &+ (\underline{\mathbf{w}} \times \mathbf{w}_d \times \mathbf{w}] - \mathbf{w}]^{[2]} \cdot \underline{\mathbf{w}}^{[2]}) e^{-j2\pi fT} \\ &+ (\mathbf{w}] \times \mathbf{w}_d \times \underline{\mathbf{w}} - \mathbf{w}]^{[2]} \cdot \underline{\mathbf{w}}^{[2]}) e^{+j2\pi fT}\} \cdot \mathbf{R}^*(f)].\end{aligned} \tag{96}$$

We illustrate these results for the binary case.

---

† The following vector relations may be established by inspection:

$$\mathbf{a}] \cdot \underline{\mathbf{b}} = \mathbf{a}] \times \underline{\mathbf{b}} = \underline{\mathbf{b}} \times \mathbf{a}].$$

‡ $\mathbf{b}_{k+n}$ and $\mathbf{b}_k$ also become independent as $n \to \infty$, because the $\mathbf{b}_k$ are unit basis vectors (Ref. 10).

6.1 Independent, binary signal pulses: $M = 1$

$\mathbf{R}(f)$ in (83) now contains four components, the Fourier transforms of the components of (56). We have

$$\underline{\mathbf{w}}_1 = [w_1 \; w_2], \quad \mathbf{w}_d = \begin{bmatrix} w_1 & 0 \\ 0 & w_2 \end{bmatrix} \tag{97}$$

$$\underline{\mathbf{w}}_1^{[2]} = [w_1^2 \; w_1 w_2 \; w_1 w_2 \; w_2^2] \tag{98}$$

$$\mathbf{w}_d^{[2]} = \begin{bmatrix} w_1^2 & 0 & 0 & 0 \\ 0 & w_1 w_2 & 0 & 0 \\ 0 & 0 & w_1 w_2 & 0 \\ 0 & 0 & 0 & w_2^2 \end{bmatrix} \tag{99}$$

$$\mathbf{w}]^{[2]} \cdot \underline{\mathbf{w}}_1^{[2]} = \begin{bmatrix} w_1^4 & w_1^3 w_2 & w_1^3 w_2 & w_1^2 w_2^2 \\ w_1^3 w_2 & w_1^2 w_2^2 & w_1^2 w_2^2 & w_1 w_2^3 \\ w_1^3 w_2 & w_1^2 w_2^2 & w_1^2 w_2^2 & w_1 w_2^3 \\ w_1^2 w_2^2 & w_1 w_2^3 & w_1 w_2^3 & w_2^4 \end{bmatrix} \tag{100}$$

$$\underline{\mathbf{w}}_1 \times \mathbf{w}_d \times \mathbf{w}] = \begin{bmatrix} w_1^3 & 0 & w_1^2 w_2 & 0 \\ w_1^2 w_2 & 0 & w_1 w_2^2 & 0 \\ 0 & w_1^2 w_2 & 0 & w_1 w_2^2 \\ 0 & w_1 w_2^2 & 0 & w_2^3 \end{bmatrix} \tag{101}$$

$$\mathbf{w}] \times \mathbf{w}_d \times \underline{\mathbf{w}}_1 = (\underline{\mathbf{w}}_1 \times w_d \times \mathbf{w}])'. \tag{102}^{\dagger}$$

Equations (98) to (102) substituted in (94) to (96) yield the final results for independent, binary signal pulses.

To illustrate, we write out a few terms of the matrix contained in $\{\ \}$ in (96), for the continuous spectrum in the binary case:[15]

$$\begin{aligned} \{\ \}_{11} &= w_1^2(1 - w_1^2)(1 + 2w_1 \cos 2\pi fT), \\ \{\ \}_{12} &= w_1^2 w_2 e^{+j2\pi fT} - w_1^3 w_2(1 + 2 \cos 2\pi fT), \\ &\vdots \\ \{\ \}_{44} &= \cdots. \end{aligned} \tag{103}$$

Writing out even the present simplest overlapping case produces an awful mess. Consequently, in the examples presented in this paper the digital computer is programmed to work directly with (96) or its generalization (116), performing matrix operations (both ordinary and Kronecker matrix multiplication) directly, rather than entering expressions such as (103). In this way, quite complicated cases involving multilevel signal pulses overlapping several time slots may be simply treated.

† See footnote, p. 908.

The general results for $K = 2$, (94) to (96), require the signal pulses to be less than two time slots in duration (82). Therefore, they must apply when the signal pulses are restricted to a single time slot, i.e., when the stronger condition (63) is satisfied, and must then reduce to the results for $K = 1$, (66), (67), and (72). This reduction is demonstrated in Appendix C.

VII. PSK WITH INDEPENDENT OVERLAPPING SIGNAL PULSES: GENERAL K

Finally, assume that the signal pulses occupy at most K time slots, so no more than K signal pulses overlap; $\mathbf{g}(t)$ is now given by (58). $\mathbf{r}(t)$ is given by (59) to (62), and $\mathbf{R}(f)$ by (160) and (161).

The $\mathbf{b}_k$ are given by (60) or (61); the mean and covariance of $\mathbf{b}_k$ are found from (32) to (37) and (149) to (153), assuming throughout that signal pulses in different time slots are independent, as in (70) to (71).

For the mean,

$$\underline{\beta} = \langle \underline{\mathbf{b}_k} \rangle = \prod_{i \times} \langle \underline{\mathbf{a}_{k+i}} \rangle \tag{104}$$

by the independence of the $\mathbf{a}_k$. The limits over the $\prod_{\times}$, given in (60) or (61) for K odd or even respectively, extended over K factors in either case. Thus,

$$\underline{\beta} = \underline{\mathbf{w}^{[K]}}. \tag{105}$$

For the covariance (see footnote, p. 908):

$$\begin{aligned} \tilde{\mathbf{\Phi}}_{\mathbf{b}}(n) &\equiv \langle \mathbf{b}_{k+n}] \cdot \underline{\mathbf{b}_k} \rangle \\ &= \langle (\prod_{i \times} \mathbf{a}_{k+n+i}]) \cdot (\prod_{i \times} \underline{\mathbf{a}_{k+i}}) \rangle \\ &= \langle \prod_{i \times} (\mathbf{a}_{k+n+i}] \cdot \underline{\mathbf{a}_{k+i}}) \rangle, \end{aligned} \tag{106}$$

the $\prod_{\times}$ being taken over K factors as given by either (60) or (61). By stationarity, (106) is independent of k; consequently, for both even and odd cases

$$\begin{aligned} \tilde{\mathbf{\Phi}}_{\mathbf{b}}(n) &\equiv \langle \mathbf{b}_{k+n}] \cdot \underline{\mathbf{b}_k} \rangle \\ &= \left\langle \left(\prod_{i=1 \times}^{K} \mathbf{a}_{n+i}] \right) \cdot \left(\prod_{i=1 \times}^{K} \underline{\mathbf{a}_i} \right) \right\rangle \\ &= \left\langle \prod_{i=1 \times}^{K} (\mathbf{a}_{n+1}] \cdot \underline{\mathbf{a}_i}) \right\rangle \cdot \end{aligned} \tag{107}$$

First, for $n = 0$, from the third line of (107) and the independence of the $\mathbf{a}_k$,

$$\tilde{\mathbf{\Phi}}_{\mathrm{b}}(0) = \prod_{i=1}^{K}{}_{\times} \langle \mathbf{a}_i \rceil \cdot \underline{\mathbf{a}_i} \rangle = \mathbf{w}_d^{[K]}. \tag{108}$$

Next consider $n = 1$. From the third line of (107) (see footnote, p. 915),

$$\begin{aligned} \tilde{\mathbf{\Phi}}_{\mathrm{b}}(1) &= \left\langle \prod_{i=1}^{K}{}_{\times} (\underline{\mathbf{a}_i} \times \mathbf{a}_{i+1} \rceil) \right\rangle \\ &= \langle \underline{\mathbf{a}_1} \rangle \times \left\{ \prod_{i=1}^{K}{}_{\times} \langle \mathbf{a}_i \rceil \cdot \underline{\mathbf{a}_i} \right\} \times \langle \mathbf{a}_{K+1} \rceil \rangle \\ &= \underline{\mathbf{w}} \times \mathbf{w}_d^{[K-1]} \times \mathbf{w} \rceil, \end{aligned} \tag{109}$$

the second line again following from the independence of the $\mathbf{a}_k$.

For $n = 2$, proceeding as above:

$$\begin{aligned} \tilde{\mathbf{\Phi}}_{\mathrm{b}}(2) &= \left\langle \prod_{i=1}^{K}{}_{\times} (\underline{\mathbf{a}_i} \times \mathbf{a}_{i+2} \rceil) \right\rangle \\ &= \langle \underline{\mathbf{a}_1} \rangle \times \left\langle \prod_{i=2}^{K}{}_{\times} (\mathbf{a}_{i+1} \rceil \times \underline{\mathbf{a}_i}) \right\rangle \times \langle \mathbf{a}_{K+2} \rceil \rangle \\ &= \langle \underline{\mathbf{a}_1} \rangle \times \left\langle \prod_{i=2}^{K}{}_{\times} (\underline{\mathbf{a}_i} \times \mathbf{a}_{i+1} \rceil) \right\rangle \times \langle \mathbf{a}_{K+2} \rceil \rangle \\ &= \langle \underline{\mathbf{a}_1} \rangle \times \langle \underline{\mathbf{a}_2} \rangle \times \left\{ \prod_{i=3}^{K}{}_{\times} \langle \mathbf{a}_i \rceil \cdot \underline{\mathbf{a}_i} \right\} \times \langle \mathbf{a}_{K+1} \rceil \rangle \times \langle \mathbf{a}_{K+2} \rceil \rangle \\ &= \underline{\mathbf{w}}^{[2]} \times \mathbf{w}_d^{[K-2]} \times \mathbf{w} \rceil^{[2]}. \end{aligned} \tag{110}$$

By induction:

$$\begin{aligned} \tilde{\mathbf{\Phi}}_{\mathrm{b}}(3) &= \underline{\mathbf{w}}^{[3]} \times \mathbf{w}_d^{[K-3]} \times \mathbf{w} \rceil^{[3]} \\ &\vdots \\ \tilde{\mathbf{\Phi}}_{\mathrm{b}}(K-1) &= \underline{\mathbf{w}}^{[K-1]} \times \mathbf{w}_d \times \mathbf{w} \rceil^{[K-1]} \\ \tilde{\mathbf{\Phi}}_{\mathrm{b}}(K) &= \underline{\mathbf{w}}^{[K]} \times \mathbf{w} \rceil^{[K]}. \end{aligned} \tag{111}$$

Next, from the second line of (107) and the independence of the $\mathbf{a}_K$,

$$\tilde{\mathbf{\Phi}}_{\mathrm{b}}(n) = \mathbf{w} \rceil^{[K]} \cdot \underline{\mathbf{w}}^{[K]}, \quad n \geqq K. \tag{112}$$

This result is of course consistent with the final line of (111) (see footnote, p. 915). Finally,

$$\tilde{\mathbf{\Phi}}_{\mathrm{b}}(n) = \tilde{\mathbf{\Phi}}'_{\mathrm{b}}(-n). \tag{113}$$

From these results the line component is:

$$v_l(t) = \frac{1}{T}\,\underline{\mathbf{w}}^{[K]} \cdot \sum_{n=-\infty}^{\infty} \mathbf{R}\left(\frac{n}{T}\right)\Big] e^{jn2\pi t/T}; \tag{114}$$

$$\mathbf{P}_{v_l}(f) = \frac{1}{T^2}\,|\underline{\mathbf{w}}^{[K]} \cdot \mathbf{R}(f)]|^2 \sum_{n=-\infty}^{\infty} \delta\left(f - \frac{n}{T}\right). \tag{115}$$

The continuous spectrum is:

$$\begin{aligned}\mathbf{P}_{v_c}(f) = \frac{1}{T}\,\underline{\mathbf{R}(f)} \cdot \{&(\mathbf{w}_d^{[K]} - \mathbf{w}]^{[K]} \cdot \underline{\mathbf{w}}^{[K]}) \\ &+ \sum_{n=1}^{K-1} (\underline{\mathbf{w}}^{[n]} \times \mathbf{w}_d^{[K-n]} \times \mathbf{w}]^{[n]} - \mathbf{w}]^{[K]} \cdot \underline{\mathbf{w}}^{[K]}) e^{-jn2\pi fT} \\ &+ \sum_{n=1}^{K-1} (\mathbf{w}^{[n]} \times \mathbf{w}_d^{[K-n]} \times \underline{\mathbf{w}}^{[n]} - \mathbf{w}]^{[K]} \cdot \underline{\mathbf{w}}^{[K]}) e^{+jn2\pi fT}\} \\ &\cdot \mathbf{R}^*(f)]. \end{aligned} \tag{116}$$

If we set $K = 2$ in (114) to (116), these results agree with those of Section VI. If the signal pulses are restricted to a smaller number of time slots $\tilde{K} < K$, the present results reduce correctly to those appropriate for $\tilde{K}$; this reduction is shown for $\tilde{K} = 1$, $K = 2$ in Appendix C, but the general case is left as an exercise for the reader.

VIII. EXAMPLES

We now consider a number of examples of computing spectra of multiphase PSK systems, subject to the following assumptions:

(*i*) The number of phase levels is a power of 2,

$$M = 2^N, \quad N \text{ an integer}. \tag{117}$$

(*ii*) The M signaling pulses have a common shape, and the M phase levels (peak phase modulations) are equally spaced.

$$\underline{\mathbf{g}(t)} = \frac{\pi}{M}\,[1 \;\; 3 \;\cdots\; (2M-1)]g(t), \tag{118}$$

$$g(t)_{\max} = 1. \tag{119}$$

Figure 3 shows vector diagrams of the peak phase modulations for $M = 2$, 4, and 8. We also assume that $g(t)$ is symmetric,

$$\begin{aligned} g(t) &= g(-t), \quad K \text{ even}, \\ g(t + T/2) &= g(-t + T/2), \quad K \text{ odd}, \end{aligned} \tag{120}$$

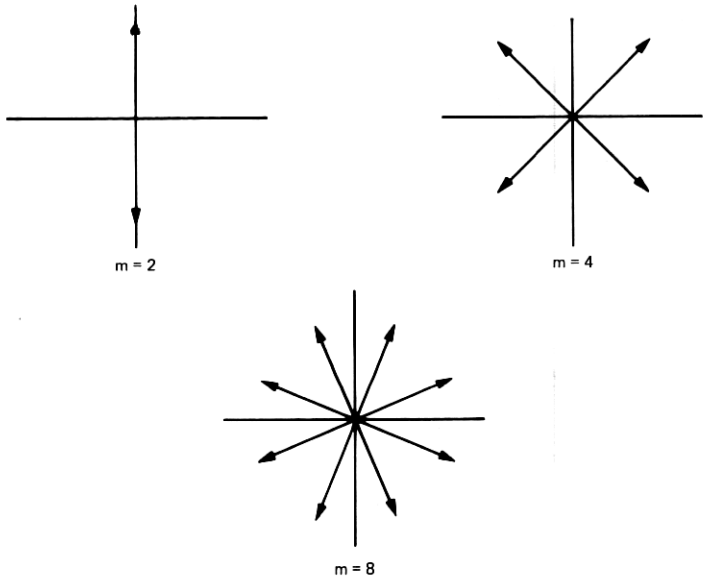

Fig. 3—Peak phase modulation for PSK with equally spaced levels.

with maximum at

$$t = 0, \quad K \text{ even},$$
$$t = \frac{T}{2}, \quad K \text{ odd}. \tag{121}$$

(*iii*) Signal pulses in different time slots are statistically independent, and all signal pulses are equally likely;

$$\mathbf{w}] = \frac{1}{M}\,\mathbf{1}], \qquad \mathbf{w}_d = \frac{1}{M}\,\mathbf{I}, \tag{122}$$

where $\mathbf{I}$ is the identity matrix of order M.

As a consequence of (118) and (122), we can show that $\mathbf{P}_v(f)$ is symmetric, that is

$$\mathbf{P}_v(f) = \mathbf{P}_v(-f). \tag{123}$$

8.1 Rectangular nonoverlapping signal pulses

If $g(t)$ is a rectangular pulse (see Fig. 4) of duration $\eta \leqq T$,

$$g(t) = \begin{cases} 1, & \dfrac{T-\eta}{2} < t \leqq \dfrac{T+\eta}{2}, \quad 0 < \eta \leqq T, \\ 0, & \text{otherwise.} \end{cases} \tag{124}$$

From (118) and (64),

$$R_i(f) = \left\{\exp\{j\frac{\pi}{M}(2i-1)\} - 1\right\}\frac{\sin \pi f\eta}{\pi f}\, e^{-j\pi fT} + \frac{\sin \pi fT}{\pi f}\, e^{-j\pi fT}, \quad i = 1, 2, \cdots, M. \tag{125}$$

The spectral density $\mathbf{P}_v(f)$ can be computed from (68), (73), and (122) with $\mathbf{R}_i(f)$ given by (125). The results can be shown to agree with those given in Refs. 4 and 6. Since this case can be treated as amplitude modulation and has been discussed extensively in Refs. 4 and 6, we shall not discuss it further in this paper.

8.2 Raised-cosine nonoverlapping signal pulses: K =1

If $g(t)$ is a raised-cosine pulse (see Fig. 5) of duration T, the pulse just fills the time slot, and

$$g(t) = \begin{cases} \frac{1}{2}\left[1 - \cos\frac{2\pi t}{T}\right], & 0 < t \leqq T \\ 0, & \text{otherwise.} \end{cases} \tag{126}$$

In this case, $\mathbf{R}(f)]$ may be evaluated either numerically or using Bessel function expansion (which again requires the use of a computer).

For $M = 2$, 4, 8, and 16, we have evaluated as above

$$\mathbf{P}_v(f) = \mathbf{P}_{vl}(f) + \mathbf{P}_{vc}(f), \tag{127}$$

with results shown in Fig. 6. We note that there is very little variation in either the discrete or the continuous spectrum when M is increased from 2 to 16. The tails of the spectrum are not shown in Fig. 6, although they are easily calculated down to the −60-dB level.

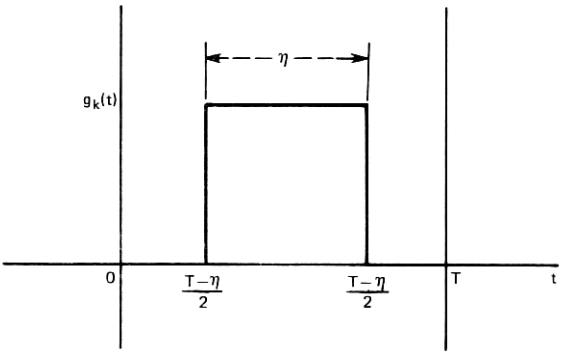

Fig. 4—Square-wave signaling of duration $\eta \leqq T$. $K = 1$.

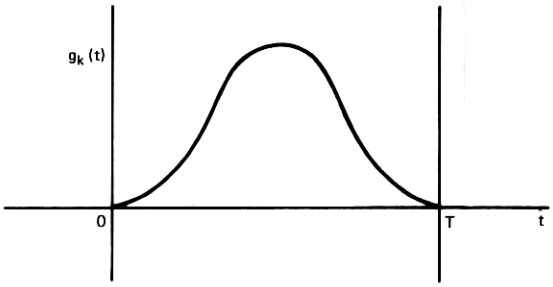

Fig. 5—Raised-cosine signaling with pulse duration T. $K = 1$.

8.3 Raised-cosine overlapping signal pulses: $K = 2$

If a raised-cosine signal pulse (see Fig. 7) just fills up two time slots,

$$g(t) = \begin{cases} \frac{1}{2}\left[1 + \cos\frac{\pi t}{T}\right], & -T < t \leqq T, \\ 0, & \text{otherwise}, \end{cases} \tag{128}$$

$K = 2$, and two signal pulses overlap.

In this case, $\mathbf{P}_{v_i}(f)$ and $\mathbf{P}_{v_c}(f)$ are given by (95), (96), (122). Using a digital computer, $\mathbf{P}_v(f)$ has been determined for $M = 2$, 4, 8, and 16, and the results plotted in Fig. 8. Again, it may be noted that there is not very much variation in either the discrete or the continuous spectra when the number of phase levels M is increased from 2 to 16.

Comparing Figs. 6 and 8, we observe that the power in the line components in a PSK system with overlapping signal pulses is smaller than the power in the lines with nonoverlapping pulses. Also, for the same signaling rates, the principal portion of the continuous part of the spectrum with $K = 2$ is narrower than that with $K = 1$. The tails of $\mathbf{P}_v(f)$ were calculated down to -60 dB even though they are not shown in Fig. 8.

In Fig. 9, for $M = 4$, and raised-cosine wave signaling, we plot the spectral density $\mathbf{P}_v(f)$ when the amount of overlap is increased from zero to one time slot. Specifically, we assume that

$$g(t) = \begin{cases} \frac{1}{2}\left[1 + \cos\frac{\pi t}{\beta T}\right], & -\beta T < t \leqq \beta T, \quad 0.5 \leqq \beta \leqq 1, \\ 0, & \text{otherwise}. \end{cases} \tag{129}$$

Note that $K = 1$ when $\beta = 0.5$, and $K = 2$ when $0.5 < \beta \leqq 1$. Figure 9 shows that there is a gradual reduction of power in the line

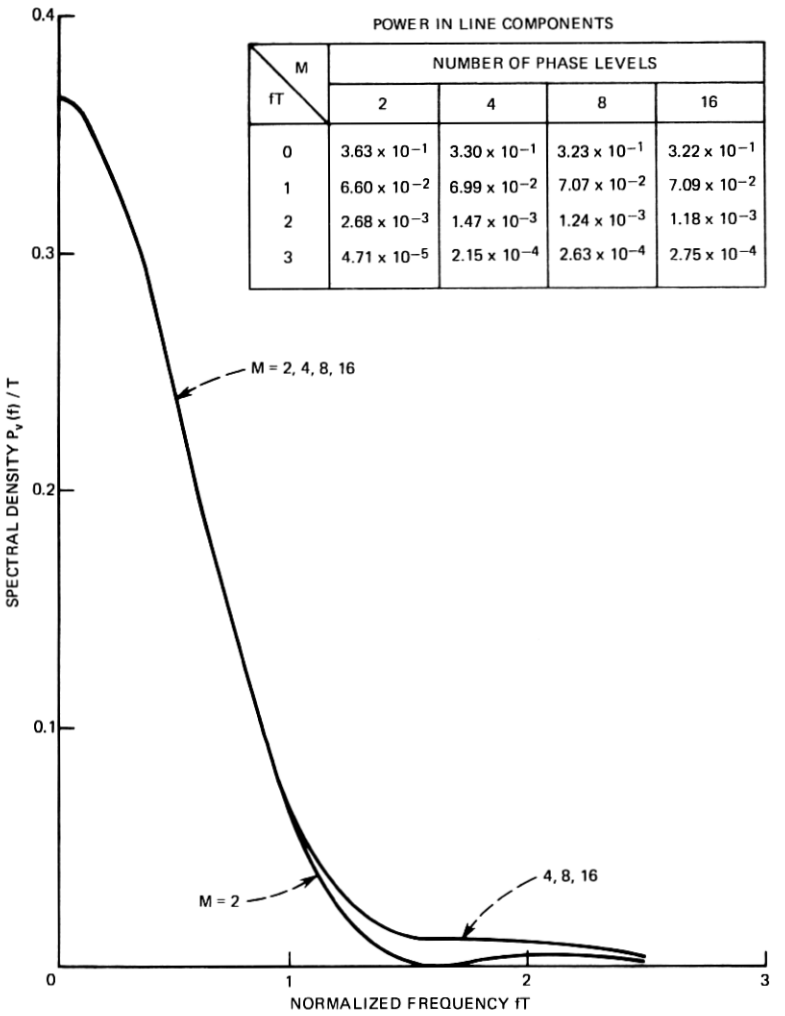

Fig. 6—Spectral density of binary, quaternary, octonary, and 16-ary PSK systems with raised-cosine signaling and pulse duration T. $K = 1$. Although the values of the spectral density for $M = 2, 4, 8$, and 16 are shown to be the same over certain segments of the range of f, they are usually different from each other, but this difference is not large enough to be shown on the linear scale in Fig. 6.

components when the overlap is increased from zero to one time slot. There is also the narrowing of the principal portion of the spectrum.

Decrease of the carrier component [$n = 0$ term in (68) or (95)] when β is increased may result from the fact that the phasors in Fig. 3 spend

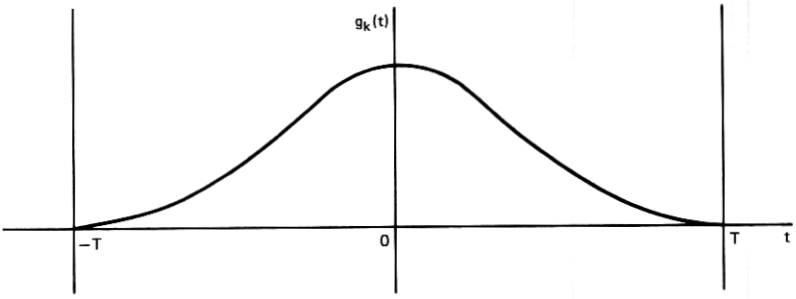

Fig. 7—Raised-cosine signaling with pulse duration $2T$. $K = 2$.

increasingly less time in the neighborhood of 0°. There are also smoother transitions between the phasors with increasing β; this probably explains the decrease in width of the main part of continuous spectrum. The narrowing of the spectral density and the reduction of the discrete spectral lines may or may not indicate better interchannel and intersymbol performance, but this remains a subject for future investigation.

IX. SUMMARY AND CONCLUSIONS

Matrix methods have been used to express the spectral density of a sinusoidal carrier phase modulated by a pulse train with a finite pulse duration. Arbitrary pulse shapes may be used for M-ary digital signaling and they may overlap over a finite number of signaling intervals.

If the pulse duration is one signaling interval, our results give the spectral density even though successive symbols are correlated. If the pulse duration is more than one signaling interval, we assume that symbols transmitted during different time slots are statistically independent; the case of correlated symbols may be considered by extension of the present work, but the required statistical description of the modulation $\mathbf{a}_k$ will be more complicated. For example, if $K = 2$, in addition to $\langle \mathbf{a}_k] \rangle$, $\langle \mathbf{a}_k] \times \underline{\mathbf{a}_l} \rangle$, we need to know $\langle \mathbf{a}_i] \times \mathbf{a}_k] \times \underline{\mathbf{a}_l} \times \underline{\mathbf{a}_m} \rangle$, the fourth order statistics of $\mathbf{a}_k$, to determine the spectral density from our methods.

The spectral density has a compact Hermitian form suitable for numerical computation by a digital computer. The associated Hermitian matrix is a function of only the symbol probabilities, and the column matrix associated with the Hermitian form is the Fourier transform of certain time functions related to the signaling pulses. The computations presented in this paper for binary, quaternary, octonary,

POWER IN LINE COMPONENTS

fT \ M	NUMBER OF PHASE LEVELS			
	2	4	8	16
0	5.57×10^{-2}	3.73×10^{-2}	3.39×10^{-2}	3.31×10^{-2}
1	1.56×10^{-2}	1.13×10^{-2}	1.04×10^{-2}	1.02×10^{-2}
2	4.90×10^{-5}	1.03×10^{-4}	1.12×10^{-4}	1.14×10^{-4}
3	2.23×10^{-8}	1.88×10^{-7}	2.58×10^{-7}	2.78×10^{-7}

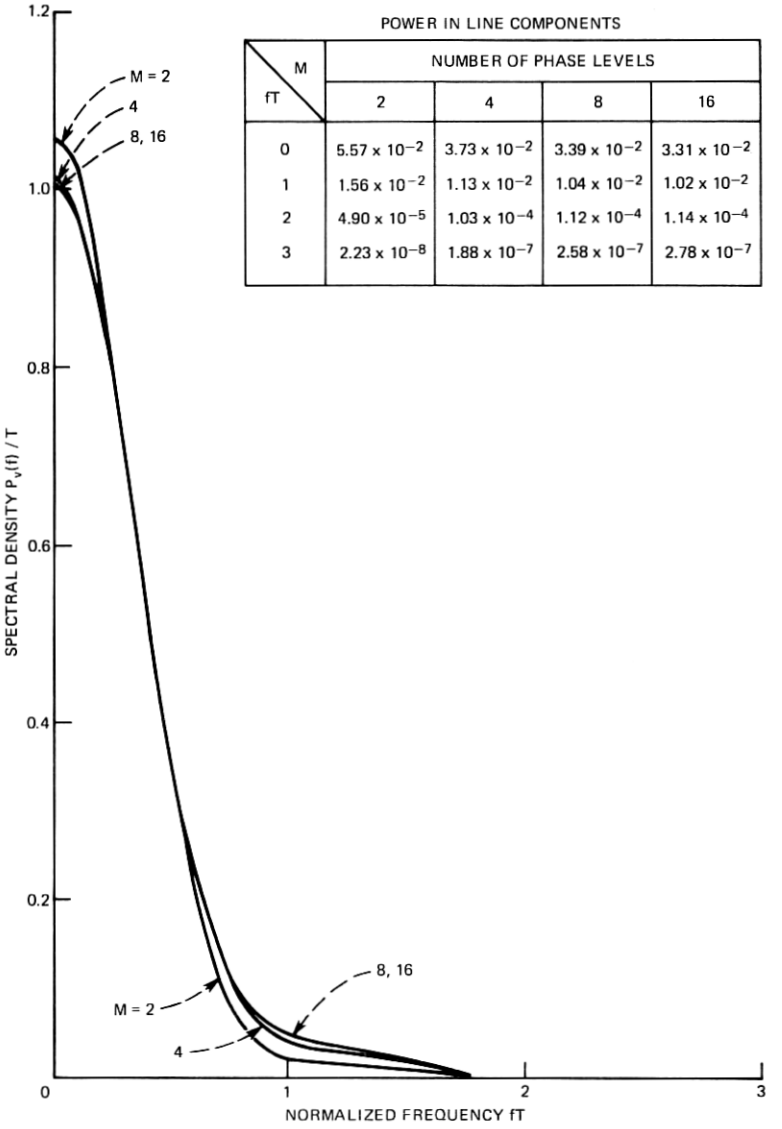

Fig. 8—Spectral density of binary, quaternary, octonary, and 16-ary PSK systems with raised-cosine signaling and pulse duration $2T$. $K = 2$. Although the values of the spectral density for $M = 2$, 4, 8, and 16 are shown to be the same over certain segments of the range of f, they are usually different from each other, but this difference is not large enough to be shown on the linear scale in Fig. 8.

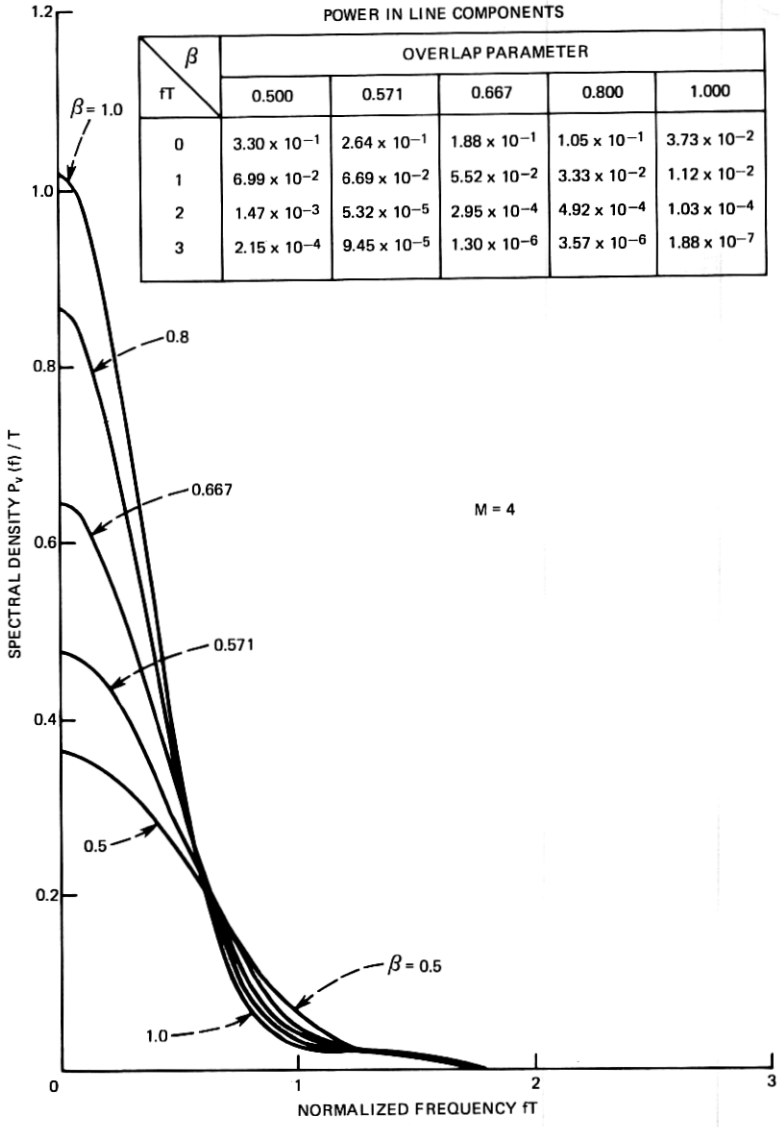

Fig. 9—Spectral density of quaternary PSK system with raised-cosine signaling and pulse duration $2\beta T$, $0.5 \leqq \beta \leqq 1$. When $\beta = 0.5$, $K = 1$, the pulse fills up just one time slot and the spectral density is as shown in Fig. 6. When $\beta = 1$, $K = 2$, the pulse fills up just two time slots, and the spectral density is as shown in Fig. 8. Although the values of the spectral density for $\beta = 0.5$, 0.571, 0.667, 0.8, and 1.0 are shown to be the same over certain segments of the range of f, they are usually different from each other, but this difference is not large enough to be shown on the linear scale in Fig. 9. Note that when $\beta = 0.5$, 0.571, 0.667, 0.8, and 1.0, $1/\beta = 2$, 1.75, 1.5, 1.25, and 1.0.

and 16-ary PSK systems do not consume very much computer time and are quite inexpensive.

Extraction of a timing wave is often essential in the detection and regeneration of digital signals. In a self-timed digital system not containing a timing wave, the wave is extracted from an incoming pulse stream by a nonlinear processing of the signal. For example, the incoming pulse stream may be passed through a square-law rectifier and a linear narrow-band filter to get the timing wave. We would like to note here that the methods given in this paper can be extended to determine the spectral density of the output of a nonlinear device whose input is a random time pulse train of the form (16) or (42). The results presented here apply to the particular nonlinearity exp $j(\cdot)$; other nonlinear functions are treated in a similar manner.

X. ACKNOWLEDGMENT

We would like to thank Wanda L. Mammel for carrying out the computations reported in this paper, and also for her help in determining the numerical accuracy of the results.

APPENDIX A

Spectra of Complex and Real PSK Waves

From (1) written in complex form, the covariance of the real wave $x(t)$ is

$$\begin{aligned}\Phi_x(\tau) &= \overline{\Phi_x(t, \tau)} \\ &= \tfrac{1}{4}\{e^{j2\pi f_c\tau}\Phi_v(\tau) + e^{-j2\pi f_c\tau}\Phi_v^*(\tau) + e^{j2\pi f_c\tau}\overline{e^{j4\pi f_c t}\Phi_{vv^*}(t, \tau)} \\ &\qquad + e^{-j2\pi f_c\tau}\overline{e^{-j4\pi f_c t}\Phi_{vv^*}^*(t, \tau)}\}, \qquad (130)\end{aligned}$$

where the cross-variance is given by

$$\Phi_{vv^*}(t, \tau) = \langle v(t + \tau)v(t)\rangle = \langle e^{j[\phi(t+\tau)+\phi(t)]}\rangle. \qquad (131)$$

Now $\Phi_{vv^*}(t, \tau)$, with τ regarded as a parameter, is periodic in t with period T;

$$\Phi_{vv^*}(t + T, \tau) = \Phi_{vv^*}(t, \tau). \qquad (132)$$

This follows from the assumed strict stationarity of the s_k of (2). Then we may write

$$\Phi_{vv^*}(t, \tau) = \sum_{n=-\infty}^{\infty} \varphi_n(\tau)e^{jn2\pi t/T}. \qquad (133)$$

Substituting in the time average quantity of (130) and interchanging the order of summation and integration,

$$\overline{e^{j4\pi f_c t}\Phi_{vv^*}(t,\tau)} = \sum_{n=-\infty}^{\infty} \varphi_n(\tau) \lim_{A\to\infty} \frac{1}{2A} \int_{-A}^{A} e^{j2\pi[2f_c+(n/T)]t}dt$$

$$= \sum_{n=-\infty}^{\infty} \varphi_n(\tau) \lim_{A\to\infty} \frac{\sin 2\pi[2f_c + (n/T)]A}{2\pi[2f_c + (n/T)]A}. \tag{134}$$

The $\lim_{A\to\infty} \to 0$ if $2f_c + (n/T) \neq 0$ for every integer n, i.e., if twice the carrier frequency is not a precise multiple of the modulation frequency $1/T$. Under this condition, (130) and (134) yield (5).

Next, assume that $\mathbf{P}_v(f)$ is strictly band-limited;

$$\mathbf{P}_v(f) = 0, \quad |f| \geqq f_c. \tag{135}$$

Then $\mathbf{P}_v(f - f_c)$ and $\mathbf{P}_v(-f - f_c)$, the two terms appearing in (5), do not overlap. Now define

$$\nu(t) \equiv e^{j2\pi f_c t}v(t). \tag{136}$$

Then

$$\begin{aligned} &\Phi_\nu(t,\tau) = e^{j2\pi f_c \tau}\Phi_v(t,\tau); \quad \Phi_\nu(\tau) = e^{j2\pi f_c\tau}\Phi_v(\tau). \\ &\mathbf{P}_\nu(f) = \mathbf{P}_v(f - f_c); \quad \mathbf{P}_{\nu^*}(f) = \mathbf{P}_v(-f - f_c). \end{aligned} \tag{137}$$

Therefore, subject to (135)

$$\begin{aligned} &\mathbf{P}_\nu(f) = 0, && f \leqq 0. \\ & && f \geqq 2f_c. \\ & && f \leqq -2f_c. \\ &\mathbf{P}_{\nu^*}(f) = 0, && f \geqq 0. \end{aligned} \tag{138}$$

Now the cross-variance of $\nu(t)$ and $\nu^*(t)$ is

$$\Phi_{\nu\nu^*}(\tau) = \overline{\Phi_{\nu\nu^*}(t,\tau)} = e^{j2\pi f_c\tau}\,\overline{e^{j4\pi f_c t}\Phi_{vv^*}(t,\tau)}, \tag{139}$$

where Φ_{vv^*} is given by (131). The Fourier transform of (139) is the corresponding cross-spectrum $\mathbf{P}_{\nu\nu^*}(f)$. Since the two spectra $\mathbf{P}_\nu(f)$ and $\mathbf{P}_{\nu^*}(f)$ do not overlap by (138), the cross-spectrum $\mathbf{P}_{\nu\nu^*}(f)$ must be identically zero,[16] and hence also the cross-variance;

$$\Phi_{\nu\nu^*}(\tau) = 0, \quad \mathbf{P}_v(f) = 0 \quad \text{for} \quad |f| \geqq f_c. \tag{140}$$

Substituting (139) and (140) into (130) and taking the Fourier transform,

$$\mathbf{P}_x(f) = \tfrac{1}{4}\mathbf{P}_v(f - f_c) + \tfrac{1}{4}\mathbf{P}_v(-f - f_c),$$
$$\mathbf{P}_v(f) = 0 \quad \text{for} \quad |f| \geqq f_c. \tag{141}$$

While $\mathbf{P}_v(f)$ will never be strictly zero, it will eventually fall off so rapidly with increasing $|f|$ that the spectral relation of (5) will be a good approximation when f_c is large enough so that the two terms do not overlap appreciably, even if $2f_c$ is an integral multiple of $1/T$.

Consider now the exceptional case of a low carrier frequency that is an integral multiple of half the modulation frequency:

$$2f_c + \frac{n_0}{T} = 0. \tag{142}$$

Then in (134) the $\lim_{A\to\infty} \to 1$ for the n_0 term, and $\to 0$ for all other terms as before. Therefore, (130) and (134) yield

$$\Phi_x(\tau) = \tfrac{1}{4}e^{j2\pi f_c\tau}[\Phi_v(\tau) + \varphi_{-2f_cT}(\tau)]$$
$$+ \tfrac{1}{4}e^{-j2\pi f_c\tau}[\Phi_v^*(\tau) + \varphi_{-2f_cT}^*(\tau)], \quad 2f_cT = \text{integer}. \tag{143}$$

The exceptional case requires the evaluation of the additional quantity $\varphi_{-2f_cT}(\tau)$, $2f_cT$ = integer, where φ is defined in (133). This may be done similarly to the evaluation of $\Phi_v(\tau)$ performed in the text, but it is not undertaken here.

Finally, consider the wave of (9), with $\phi(t)$ given by (2), with the carrier and modulation phases ϕ_0 and t_0 independent random variables, independent of the modulation. Equation (130) is replaced by

$$\Phi_x(\tau) = \tfrac{1}{4}\{e^{j2\pi f_c\tau}\Phi_v(\tau) + e^{-j2\pi f_c\tau}\Phi_v^*(\tau)$$
$$+ e^{j2\pi f_c\tau}\langle e^{j2\phi_0}\rangle\langle e^{j4\pi f_ct_0}\rangle\overline{e^{j4\pi f_ct}\Phi_{vv^*}(t,\tau)}$$
$$+ e^{-j2\pi f_c\tau}\langle e^{-j2\phi_0}\rangle\langle e^{-j4\pi f_ct_0}\rangle\overline{e^{-j4\pi f_ct}\Phi_{vv^*}^*(t,\tau)}\}, \tag{144}$$

where v, Φ_v, and Φ_{vv^*} remain as given in (3), (7), (8), and (131) for $t_0 = 0$. The last two lines of (144) vanish if any of the three quantities

$$\overline{e^{j4\pi f_ct}\Phi_{vv^*}(t,\tau)}, \quad \langle e^{j2\phi_0}\rangle, \quad \langle e^{j4\pi f_ct_0}\rangle \tag{145}$$

vanish. Therefore,

$$\mathbf{P}_x(f) = \tfrac{1}{4}\mathbf{P}_v(f - f_c) + \tfrac{1}{4}\mathbf{P}_v(-f - f_c) \tag{146}$$

if any of the following conditions are satisfied:

$2f_cT \neq$ integer.

$2f_cT =$ integer, ϕ_0 is uniformly distributed over an interval

$$\pi, 2\pi, 3\pi, \cdots. \tag{147}$$

$2f_cT =$ integer, t_0 is uniformly distributed over an interval

$$\frac{T}{2f_cT}, \quad 2\frac{T}{2f_cT}, \quad 3\frac{T}{2f_cT}, \cdots.$$

The first condition is, of course, that of (5). The last two conditions show that suitably randomizing the phase of either the carrier or the modulation suffices to yield the simple spectral result of (5) when $2f_cT =$ integer.

APPENDIX B

Spectrum of a Baseband Pulse Train With Different Pulse Shapes

We determine the spectral density of (43),

$$v(t) = \sum_{k=-\infty}^{\infty} \underline{\mathbf{b}_k} \cdot \mathbf{r}(t - kT)], \tag{148}$$

by the vector analog of the corresponding derivation for a train of equally spaced pulses with similar shapes. In this appendix, the waveforms $\mathbf{r}$ for different time slots (i.e., different k) may overlap, although they do not overlap in the applications of this paper. Also, $\mathbf{b}_k$ may be complex in this appendix. It is real in the main part of the paper.

Let $\mathbf{b}_k$ in (43) and (148) be wide-sense stationary. Then, using the notation of (35) to (40):

$$\underline{\mathfrak{B}} \equiv \langle \underline{\mathbf{b}_k} \rangle. \tag{149}$$

$$\tilde{\mathbf{\Phi}}_{\mathbf{b}}(k - l) \equiv \langle \mathbf{b}_k] \cdot \underline{\mathbf{b}_l^*} \rangle. \tag{150}$$

$$\tilde{\mathbf{P}}_{\mathbf{b}}(f) = \sum_{n=-\infty}^{\infty} e^{-j2\pi fn} \tilde{\mathbf{\Phi}}_{\mathbf{b}}(n). \tag{151}$$

$$\tilde{\mathbf{\Phi}}_{\mathbf{b}}(n) = \int_{-\frac{1}{2}}^{\frac{1}{2}} \tilde{\mathbf{P}}_{\mathbf{b}}(f) e^{+j2\pi fn} df. \tag{152}$$

Further, assume that $\mathbf{b}_{k+n}$ and $\mathbf{b}_k$ become uncorrelated as $n \to \infty$:

$$\lim_{n \to \infty} \tilde{\mathbf{\Phi}}_{\mathbf{b}}(n) \equiv \tilde{\mathbf{\Phi}}_{\mathbf{b}}(\infty) = \mathfrak{B}] \cdot \underline{\mathfrak{B}^*}. \tag{153}$$

From (148),

$$\Phi_v(t, \tau) = \langle v(t + \tau)v^*(t)\rangle$$

$$= \sum_{k=-\infty}^{\infty} \sum_{l=-\infty}^{\infty} \underline{\mathbf{r}(t + \tau - kT)} \cdot \tilde{\mathbf{\Phi}}_b(k - l) \cdot \mathbf{r}^*(t - lT)]. \tag{154}$$

Since

$$\Phi_v(t + T, \tau) = \Phi_v(t, \tau), \tag{155}$$

we have

$$\Phi_v(\tau) = \overline{\Phi_v(t, \tau)} = \frac{1}{T} \int_{-T/2}^{T/2} \Phi_v(t, \tau)dt. \tag{156}$$

Substituting (154) in (156) and making the substitutions $k - l = n$ and $t - lT = t'$,

$$\Phi_v(\tau) = \frac{1}{T} \sum_{n=-\infty}^{\infty} \sum_{l=-\infty}^{\infty} \int_{-(l+\frac{1}{2})T}^{-(l-\frac{1}{2})T} \underline{\mathbf{r}(t + \tau - nT)} \cdot \tilde{\mathbf{\Phi}}_b(n) \cdot \mathbf{r}^*(t)]dt$$

$$= \frac{1}{T} \sum_{n=-\infty}^{\infty} \int_{-\infty}^{\infty} \underline{\mathbf{r}(t + \tau - nT)} \cdot \tilde{\mathbf{\Phi}}_b(n) \cdot \mathbf{r}^*(t)]dt. \tag{157}$$

The spectral density of (148) is now the Fourier transform of (157):

$$\mathbf{P}_v(f) = \int_{-\infty}^{\infty} \Phi_v(\tau)e^{-j2\pi f\tau}d\tau$$

$$= \frac{1}{T} \sum_{n=-\infty}^{\infty} \int_{-\infty}^{\infty} \int_{-\infty}^{\infty} e^{-j2\pi f\tau} \underline{\mathbf{r}(t + \tau - nT)}$$

$$\cdot \tilde{\mathbf{\Phi}}_b(n) \cdot \mathbf{r}^*(t)]dtd\tau. \tag{158}$$

The treatment differs slightly from that for the scalar case, because the order of the factors in the matrix products may not be changed. Setting $t' = t + \tau$, (158) becomes

$$\mathbf{P}_v(f) = \frac{1}{T} \sum_{n=-\infty}^{\infty} \left\{ \int_{-\infty}^{\infty} e^{-j2\pi ft'} \underline{\mathbf{r}(t' - nT)}dt' \right\} \cdot \tilde{\mathbf{\Phi}}_b(n)$$

$$\cdot \left\{ \int_{-\infty}^{\infty} e^{+j2\pi ft} \mathbf{r}^*(t)]dt \right\} \cdot \tag{159}$$

Define

$$\mathbf{R}(f)] = \underline{\mathbf{R}(f)'} \equiv \int_{-\infty}^{\infty} e^{-j2\pi ft} \mathbf{r}(t)]dt; \tag{160}$$

i.e., the elements of $\mathbf{r}(t)$ and $\mathbf{R}(f)$ are the pulse shapes and their

Fourier transforms, respectively. In applications throughout the remainder of this paper,

$$\mathbf{r}(t)\rceil = \mathbf{0}\rceil, \quad t \leqq 0, \quad t > T, \tag{161}$$

and the integral in (160) therefore takes the limits $\int_0^T$. However, the restriction of (161) is not necessary in this appendix. Substituting (160) into (159) and using (151),

$$\tilde{\mathbf{P}}_v(f) = \frac{1}{T}\underline{\mathbf{R}(f)}\cdot\tilde{\mathbf{P}}_b(fT)\cdot\mathbf{R}^*(f)\rceil, \tag{162}$$

our desired result. Eq. (162) reduces correctly to the scalar case.[17]

It is convenient to separate out the line component of $v(t)$. As in (39) and (40), the line and continuous components of (151) are, using (153),

$$\tilde{\mathbf{P}}_{bl}(f) = \mathfrak{B}\rceil\cdot\underline{\mathfrak{B}^*}\sum_{n=-\infty}^{\infty}\delta(f-n). \tag{163}$$

$$\tilde{\mathbf{P}}_{bc}(f) = \sum_{n=-\infty}^{\infty} e^{-j2\pi fn}\{\tilde{\mathbf{\Phi}}_b(n) - \mathfrak{B}\rceil\cdot\underline{\mathfrak{B}^*}\}. \tag{164}$$

The line and continuous spectral components of (148) are found by substituting (163) and (164) into (162). For the line component

$$\begin{aligned}\mathbf{P}_{vl}(f) &= \frac{1}{T^2}\underline{\mathbf{R}(f)}\cdot\mathfrak{B}\rceil\cdot\underline{\mathfrak{B}^*}\cdot\mathbf{R}^*(f)\rceil\sum_{n=-\infty}^{\infty}\delta\left(f-\frac{n}{T}\right)\\ &= \frac{1}{T^2}\,|\underline{\mathfrak{B}}\cdot\mathbf{R}(f)\rceil|^2\sum_{n=-\infty}^{\infty}\delta\left(f-\frac{n}{T}\right).\end{aligned} \tag{165}$$

The line component is composed of dc and sine waves at the signaling rate and its harmonics.

Finally, taking the expected value of (148) and using (149),

$$\langle v(t)\rangle = \underline{\mathfrak{B}}\cdot\sum_{k=-\infty}^{\infty}\mathbf{r}(t-kT)\rceil. \tag{166}$$

Then

$$\begin{aligned}\Phi_{\langle v\rangle}(t,\tau) &= \langle v(t+\tau)\rangle\langle v^*(t)\rangle\\ &= \sum_{k=-\infty}^{\infty}\sum_{l=-\infty}^{\infty}\underline{\mathbf{r}(t+\tau-kT)}\cdot\mathfrak{B}\rceil\cdot\underline{\mathfrak{B}^*}\cdot\mathbf{r}^*(t-lT)\rceil.\end{aligned} \tag{167}$$

Comparing with (154) and proceeding as above,

$$\Phi_{\langle v \rangle}(\tau) = \frac{1}{T} \sum_{n=-\infty}^{\infty} \int_{-\infty}^{\infty} \underline{\mathbf{r}(t + \tau - nT)} \cdot \underline{\beta}] \cdot \underline{\beta}^* \cdot \mathbf{r}^*(t)] dt. \quad (168)$$

Consequently, (168) is a periodic function of τ with period T. Comparing (157) and (168) as $|\tau| \to \infty$, using (153), and assuming that $\mathbf{r}(t)$ eventually falls off for large $|t|$ [the stronger assumption (161) applies throughout the rest of this paper],

$$\Phi_v(\tau) \to \Phi_{\langle v \rangle}(\tau) \quad \text{as} \quad |\tau| \to \infty. \quad (169)$$

Therefore, we may write (148) as

$$v(t) = v_l(t) + v_c(t), \quad (170)$$

where, from (166),

$$v_l(t) = \underline{\beta} \cdot \sum_{k=-\infty}^{\infty} \mathbf{r}(t - kT)]$$

$$= \frac{1}{T} \underline{\beta} \cdot \sum_{n=-\infty}^{\infty} \mathbf{R}\left(\frac{n}{T}\right)] e^{jn2\pi t/T}, \quad (171)$$

and the spectral densities of $v_l(t)$ and $v_c(t)$ are given by (165) and by substituting (164) into (162), respectively. Equation (171) contains phase information lost in (165).

The assumption of (153) follows if the vector coefficients $\mathbf{b}_k$ become independent for widely separated time slots. For the applications of this paper, the $\mathbf{b}_k$ are unit basis vectors, i.e., each $\mathbf{b}_k$ has a single component equal to unity and all other components zero. In this special case, the assumption of (153) that $\mathbf{b}_k$ in widely separated time slots are uncorrelated also guarantees independence.[10]

APPENDIX C

Simplification of PSK Spectra for $K = 2$ for Nonoverlapping Signal Pulses

We demonstrate that the $K = 2$ results, (94) to (96), which apply subject to condition (82), specialize to the $K = 1$ results (66), (67), and (72) when the stronger condition (63) is satisfied.

We distinguish the different $\mathbf{R}$'s in Sections V and VI by appending subscripts K, denoting (64) and (83) as $\mathbf{R}_1$ and $\mathbf{R}_2$, respectively. Then if, in Section VI, (82) is replaced by the stronger condition (63), (83) becomes

$$\mathbf{R}_2(f)] = \mathbf{R}_1(f)] \times \mathbf{1}], \quad (172)$$

where $\mathbf{R}_1$ is given by (64) and $\mathbf{1}$ is the M-dimensional vector with all components unity defined in (24).

Considering first (94) and (95), using (26) and (172) (see footnote, p. 908):

$$\begin{aligned}\underline{\mathbf{w}}^{[2]}\cdot\mathbf{R}_2(f)\rceil &= (\underline{\mathbf{w}}\times\underline{\mathbf{w}})\cdot(\mathbf{R}_1(f)\rceil\times\mathbf{1}\rceil)\\ &= (\underline{\mathbf{w}}\cdot\mathbf{R}_1(f)\rceil)\times(\underline{\mathbf{w}}\cdot\mathbf{1}\rceil) = \underline{\mathbf{w}}\cdot\mathbf{R}_1(f)\rceil. \end{aligned}\tag{173}$$

Substituting (173) into (94) and (95) yields (66) and (67).

Next, substituting (172) into (96), we evaluate the following resulting products using (26) and (28) (see footnote, p. 908):

$$\begin{aligned}&\underline{\mathbf{R}_2(f)}\cdot\mathbf{w}_d^{[2]}\cdot\mathbf{R}_2^*(f)\rceil\\ &\quad= (\underline{\mathbf{R}_1(f)}\times\underline{\mathbf{1}})\cdot(\mathbf{w}_d\times\mathbf{w}_d)\cdot(\mathbf{R}_1^*(f)\rceil\times\mathbf{1}\rceil)\\ &\quad= (\underline{\mathbf{R}_1(f)}\cdot\mathbf{w}_d\cdot\mathbf{R}_1^*(f)\rceil)\times(\underline{\mathbf{1}}\cdot\mathbf{w}_d\cdot\mathbf{1}\rceil)\\ &\quad= \underline{\mathbf{R}_1(f)}\cdot\mathbf{w}_d\cdot\mathbf{R}_1^*(f)\rceil.\end{aligned}\tag{174}$$

$$\begin{aligned}&\underline{\mathbf{R}_2(f)}\cdot\mathbf{w}\rceil^{[2]}\cdot\underline{\mathbf{w}}^{[2]}\cdot\mathbf{R}_2^*(f)\rceil\\ &\quad= (\underline{\mathbf{R}_1(f)}\times\underline{\mathbf{1}})\cdot(\mathbf{w}\rceil\times\mathbf{w}\rceil)\cdot(\underline{\mathbf{w}}\times\underline{\mathbf{w}})\cdot(\mathbf{R}_1^*(f)\rceil\times\mathbf{1}\rceil)\\ &\quad= (\underline{\mathbf{R}_1(f)}\cdot\mathbf{w}\rceil\cdot\underline{\mathbf{w}}\cdot\mathbf{R}_1^*(f)\rceil)\times(\underline{\mathbf{1}}\cdot\mathbf{w}\rceil\cdot\underline{\mathbf{w}}\cdot\mathbf{1}\rceil)\\ &\quad= (\underline{\mathbf{R}_1(f)}\cdot\mathbf{w}\rceil)(\underline{\mathbf{w}}\cdot\mathbf{R}_1^*(f)\rceil)\\ &\quad= |\underline{\mathbf{w}}\cdot\mathbf{R}_1(f)\rceil|^2.\end{aligned}\tag{175}$$

$$\begin{aligned}&\underline{\mathbf{R}_2(f)}\cdot(\underline{\mathbf{w}}\times\mathbf{w}_d\times\mathbf{w}\rceil)\cdot\mathbf{R}_2^*(f)\rceil\\ &\quad= (1\times\underline{\mathbf{R}_1(f)}\times\underline{\mathbf{1}})\cdot(\underline{\mathbf{w}}\times\mathbf{w}_d\times\mathbf{w}\rceil)\cdot(\mathbf{R}_1^*(f)\rceil\times\mathbf{1}\rceil\times 1)\\ &\quad= (1\cdot\underline{\mathbf{w}}\cdot\mathbf{R}_1^*(f)\rceil)\times(\underline{\mathbf{R}_1(f)}\cdot\mathbf{w}_d\cdot\mathbf{1}\rceil)\times(\underline{\mathbf{1}}\cdot\mathbf{w}\rceil\cdot 1)\\ &\quad= (\underline{\mathbf{w}}\cdot\mathbf{R}_1^*(f)\rceil)(\underline{\mathbf{R}_1(f)}\cdot\mathbf{w}\rceil)\\ &\quad= |\underline{\mathbf{w}}\cdot\mathbf{R}_1(f)\rceil|^2.\end{aligned}\tag{176}$$

Substituting (174) to (176) into (96) yields (72).

REFERENCES

1. W. R. Bennett, "Statistics of Regenerative Digital Transmission," B.S.T.J., *37*, No. 6 (November 1958), pp. 1501–1542.
2. W. R. Bennett and S. O. Rice, "Spectral Density and Autocorrelation Functions Associated with Binary Frequency Shift Keying," B.S.T.J., *42*, No. 5 (September 1963), pp. 2355–2385.
3. R. R. Anderson and J. Salz, "Spectra of Digital FM," B.S.T.J., *44*, No. 6 (July–August 1965), pp. 1165–1189.
4. L. Lundquist, "Digital PM Spectra by Transform Techniques," B.S.T.J., *48*, No. 2 (February 1969), pp. 397–411.

5. H. C. Van Den Elzen, "Calculating Power Spectral Densities for Data Signals," Proc. IEEE, *58*, No. 6 (June 1970), pp. 942–943.
6. B. Glance, "Power Spectra of Multilevel Digital Phase-Modulated Signals," B.S.T.J., *50*, No. 9 (November 1971), pp. 2857–2878.
7. J. E. Mazo and J. Salz, "Spectra of Frequency Modulation with Random Waveforms," Information and Control, *9*, No. 4 (August 1966), pp. 414–422.
8. O. Shimbo, "General Formula for Power Spectra of Digital FM Signals," Proc. IEE(GB), *113*, No. 11 (November 1966), pp. 1783–1789.
9. H. E. Rowe, *Signals and Noise in Communication Systems*, New York: D. Van Nostrand, 1965, pp. 98–119.
10. W. Feller, *An Introduction to Probability Theory and Its Applications*, 2nd edition, New York: John Wiley, 1957, p. 224, Prob. 16.
11. Ref. 9, pp. 22–25, 50–52.
12. R. Bellman, *Introduction to Matrix Analysis*, New York: McGraw-Hill, 1970, Ch. 12.
13. F. A. Graybill, *Introduction to Matrices with Applications in Statistics*, New York: Wadsworth, 1969, Section 8.8.
14. S. O. Rice, "Phase Jitter Produced by Overlapping Pulses in a Pulse Communication System," unpublished work, 1967.
15. B. Glance, "Power Spectrum of a Carrier Phase-Modulated by Polar Overlapping Pulses," unpublished work.
16. Ref. 9, pp. 49–50.
17. Ref. 9, pp. 236–237.